Next generation computational blood-brain barrier models

Dr Christian Jorgensen
Senior Lecturer
School of Medicine, Pharmacy and Biomedical Sciences
University of Portsmouth

BCADD-25, 20th Oct 2025

Christian.jorgensen@port.ac.uk

Developing blood-brain barrier models

Aims

- Build atomic-detail models of brain endothelial cell membranes
- Calculate transversal permeability
- Calculate transversal free-energies

Computing time: MARCC & Grant PSCA18012P

Maryland Advanced Research Computing Center

PITTSBURGH SUPERCOMPUTING CENTER

Searson (Johns Hopkins)

MBU (KCL)

Blood brain barrier (BBB)

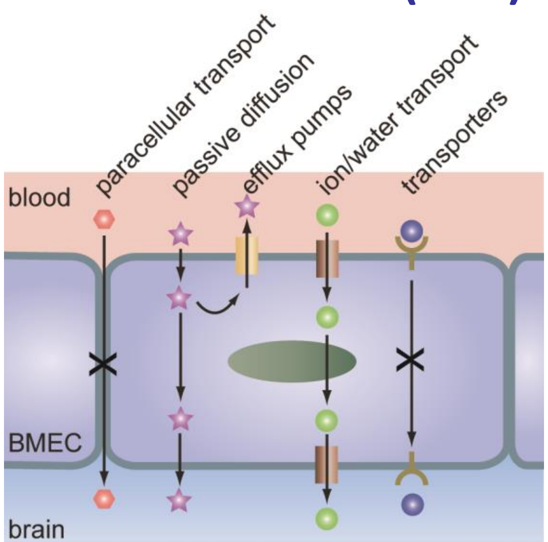

Human Brain Microvascular Endothelial Cell Models

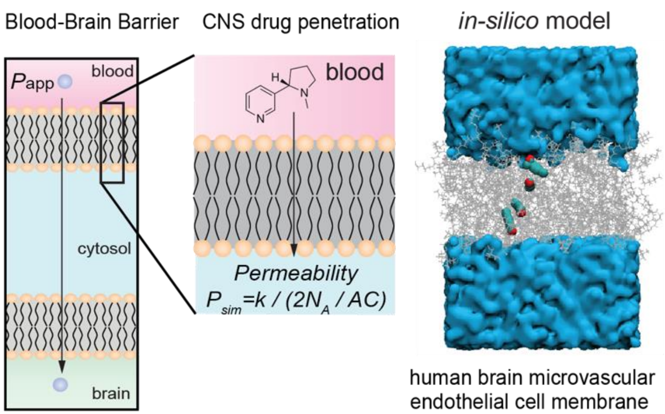

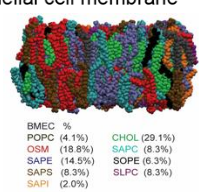

Challenge of calculating CNS passive permeability

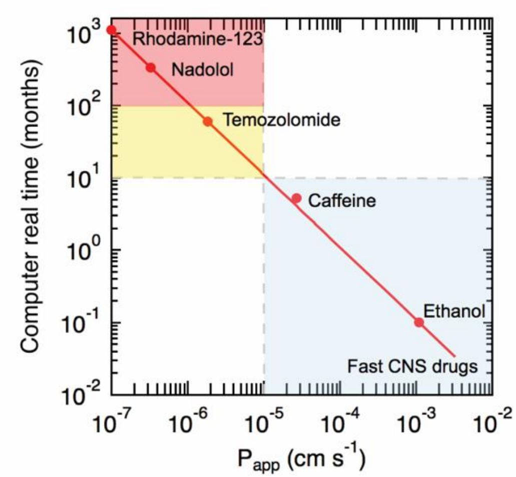

Ethanol (10^{-3} cm s^{-1})
Caffeine (10^{-5} cm s^{-1})
Temozolomide (10^{-6} cm s^{-1})
Doxorubicin (10^{-7} cm s^{-1})

BBB: 98% rejection rate of the drug space (10^{60} molecules)

C. Jorgensen, M. B. Ulmschneider, P. C. Searson, *ACS Omega*, **2022,** *7*
Y. Wang, E. Gallagher, C. Jorgensen, E. P. Troendle, D. Hu, P. C. Searson, M. B. Ulmschneider, *Sci. Rep.*, **2019**, *9*
C. Jorgensen, E. P. Troendle, J. P. Ulmschneider, P. C. Searson, M. B. Ulmschneider, *JCAMD*, **2023,** *37*
C. Jorgensen, C. *et al*. *JCIM,* **2025,** *65*

1. Lipinski's Rule of Five (Pfizer)

- MW < 500 Da
- Dipole < 5 D
- log P_{oct} < 5
- HB acceptor < 10
- HB donor < 5

C. A. Lipinski et al., *Adv. Drug Deliv. Rev*. **1997**, 23, 3-25

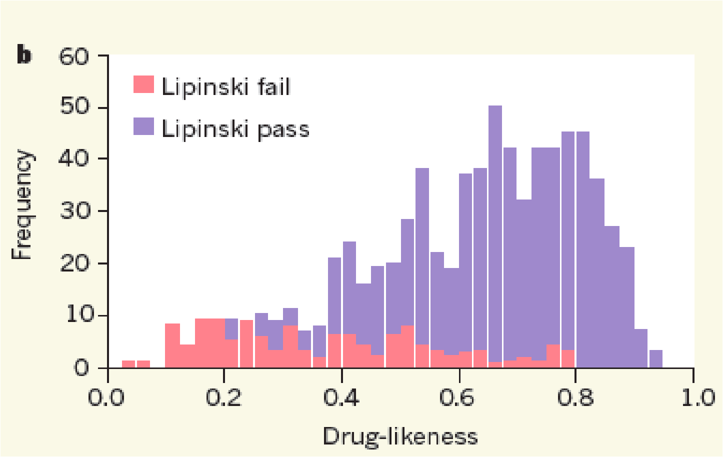

2. AI models & Bayesian pass/fail

Bayesian Pass/fail model parameters:

- Partitioning coefficent (log P_{ow})
- Van der Waals surface area
- Polar surface area
- Lipinski refinement (more parameters)

Supervised AI ML models for BBB+ / BBB-

BBB+ drugs cross. **BBB-** drugs do not cross

3. MD simulations

Quantitative high-resolution molecule-specific information

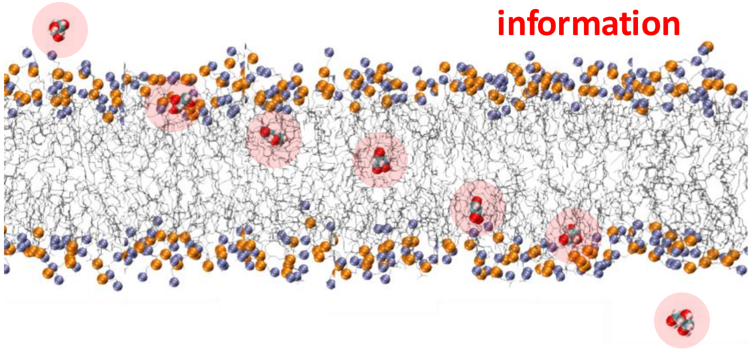

Liu et al., *Drug Metab. & Disp.*, **2004**, 32, 132-139
Martins et al., *JCIM.*, **2012**, 52, 1686-1697
Jorgensen *et al. JCIM*, **2025**, *65*
Huang, *et al. Sci. Rep.*, **2024**, 14, 9 (1), 15844.
Jia & Sosso. *JCIM*, **2024**.

Transition-based (flux-based) permeability

Flux equations

$$J = P \cdot \Delta C$$

$$P = \frac{r}{A\,C}$$

Flux (mol $m^{-2}s^{-1}$): the net number of particles *n* per unit area diffusing across a membrane with cross-section area A. Can be unidirectional or bidirectional

Permeability (cm s^{-1}): Displacement through membrane per unit time.

Challenges:

❖ Timescale renders this inaccessible for all but fastest molecules

1. Passive diffusion

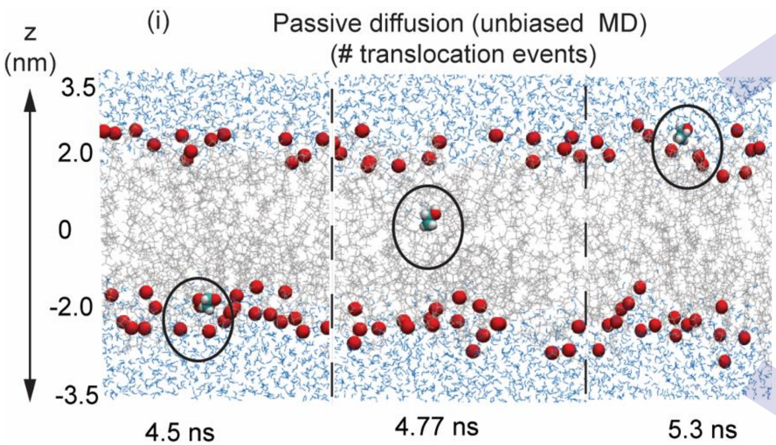

Direction of flux

- Simulations capture a bidirectional flux

$$\#_{tot} = \#_{up} + \#_{down}$$

- Experimental transwell assays capture unidirectional flux
- Total flux from simulation is divided by 2 to compare to experiment
- We assume that the transport via the cytosol is fast compared to transport across the cell membrane and negligible

2. Energetics

$$F(z) = -kT \log\ (P(z))$$

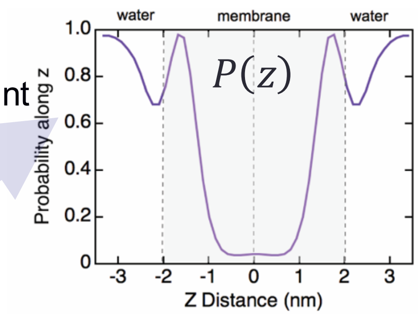

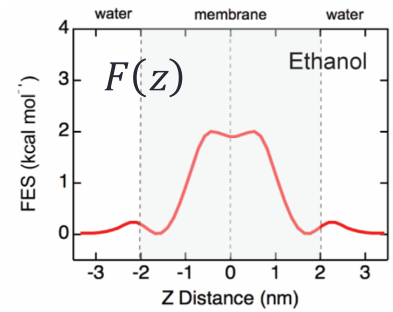

3. Transport kinetics

Rapid permeability screening of toxins and antidotes

(ii) Establish steady-state

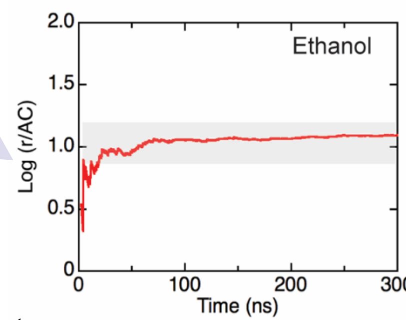

(iii) Calculate permeability

$$r = \frac{k}{N_A} = \frac{\#}{t \cdot N_A} \quad (1)$$

$$\rightarrow P_{sim} = \frac{r}{\boxed{2}AC} \quad (2)$$

#: number of permeation events
k: rate constant (ns^{-1})
r: molar rate constant (mol ns^{-1})
A: Area of lipid patch (nm^2)
C: Concentration solute (mol dm^{-3})
P: permeability (cm s^{-1})

- We can model atoms as hard spheres connected by springs (Lewitt, Warshell 1975) together with electrostatic/dispersion components.
- This turned out to be much more accurate than we thought.
- **MD simulations** generate trajectories of a system via forward time propagation of Newton's 2nd law.

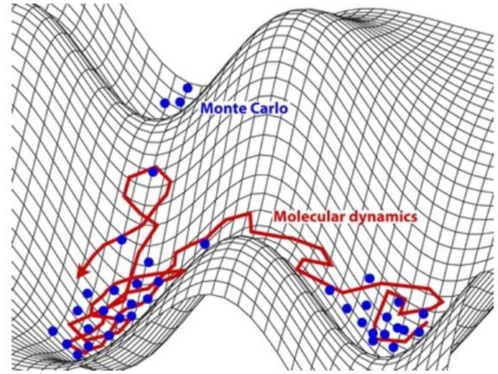

MD simulation of caffeine

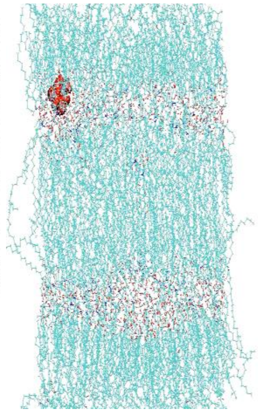

1. Workflow

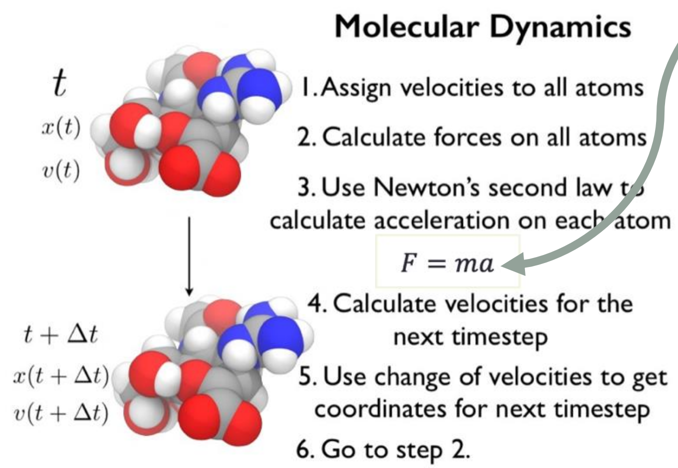

2. Force field

$F = -dU/dr$

Input the force into Newton's second law to update positions and velocities by generating the system potential energy from **bonded** and **nonbonded** contributions

Bonds

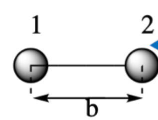

$$U(\underline{r}^N) = \sum_{\text{bonds}} K_b (b-b_0)^2 + \sum_{\text{angles}} K_\theta (\theta-\theta_0)^2 + \sum_{\text{dihedrals}} K_\chi (1+\cos(n\chi-\delta)) + \sum_{\text{Urey-Bradley}} K_{UB} (S-S_0)^2 + \sum_{\text{impropers}} K_\phi (\phi-\phi_0)^2 + \sum_{\text{Non-bonded}} \left(\varepsilon_{ij} \left[\left(\frac{R_{\min}}{r_{ij}} \right)^{12} - 2 \left(\frac{R_{\min}}{r_{ij}} \right)^{6} \right] + \frac{q_i q_j}{4\pi\varepsilon_0 r_{ij}} \right)$$

Angles

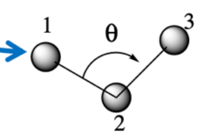

Dihedral

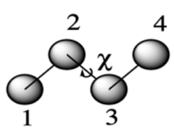

Improper Dihedral

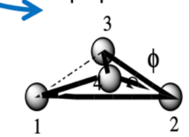

Non–bonded

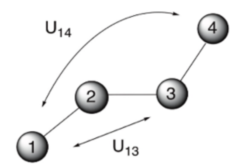

Levitt, Warshel: "Computer simulation of protein folding" *Nature*, **1975,** 253 (5494), 694-698.
Hollingsworth, Dror: "Molecular dynamics simulations for all", *Neuron*, **2019,** 99(6)

Developing an atomic model of the BBB

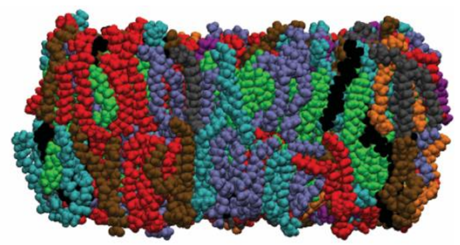

hBMEC (BBB)

hBMEC	%		
POPC	(4.1%)	CHOL	(29.1%)
OSM	(18.8%)	SAPC	(8.3%)
SAPE	(14.5%)	SOPE	(6.3%)
SAPS	(8.3%)	SLPC	(8.3%)
SAPI	(2.0%)		

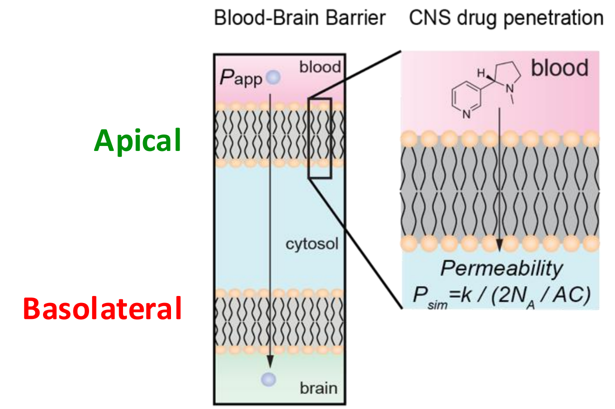

Model reproduces experimental features:

- Hydrocarbon length
- Average double bond number in lipid tails

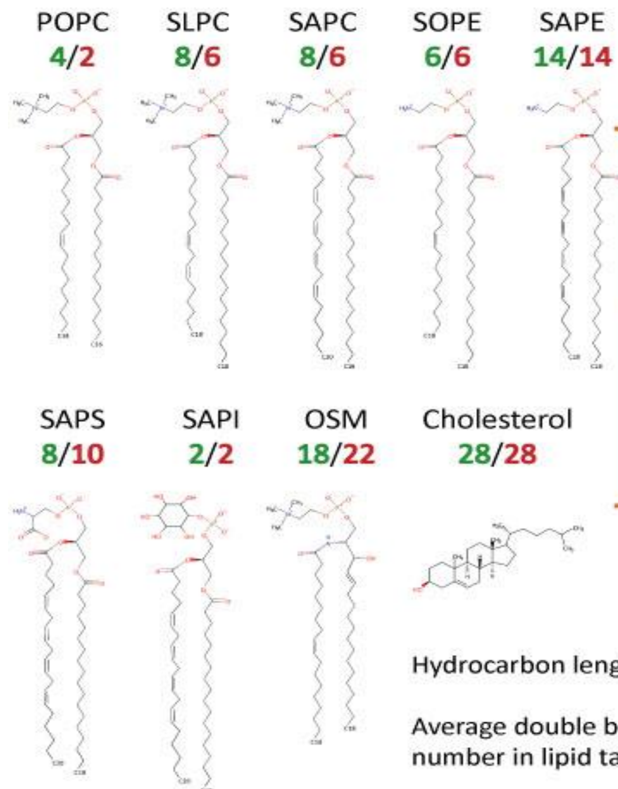

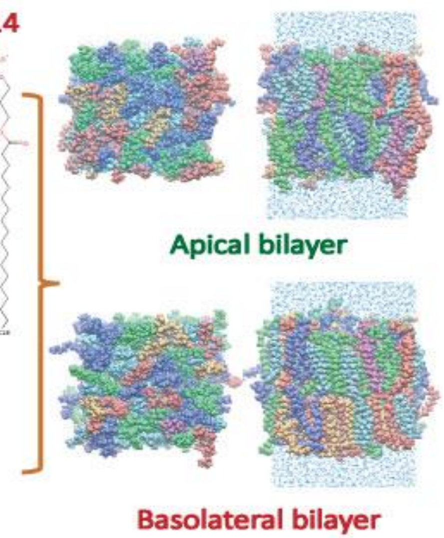

	Model	Exp.
Hydrocarbon length:	18.4 C	18.4 C
Average double bond number in lipid tails:	1.45	1.55

Lipid composition: Bénistant et al. *J. Lipid Res.*, **1995**, 36
Y. Wang, E. Gallagher, C. Jorgensen, E. P. Troendle, D. Hu, P. C. Searson, M. B. Ulmschneider, *Sci. Rep.*, **2019**, 9
C. Jorgensen, M. B. Ulmschneider, P. C. Searson, *ACS Omega*, **2022**, 7

1. Flux-based permeabilities workflow

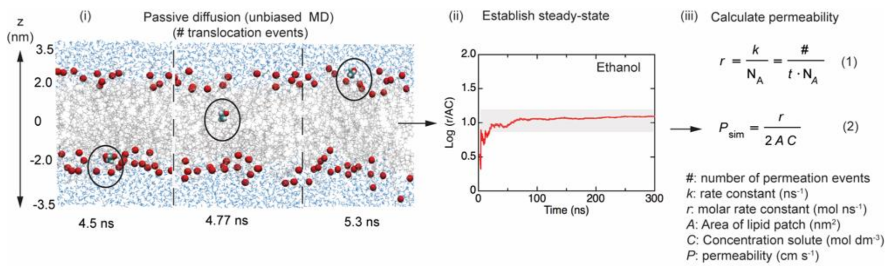

Library spans experimental permeability **10^{-7} cm s^{-1}** to **10^{-3} cm s^{-1}**

Slow Fast

2. Representative CNS drug library

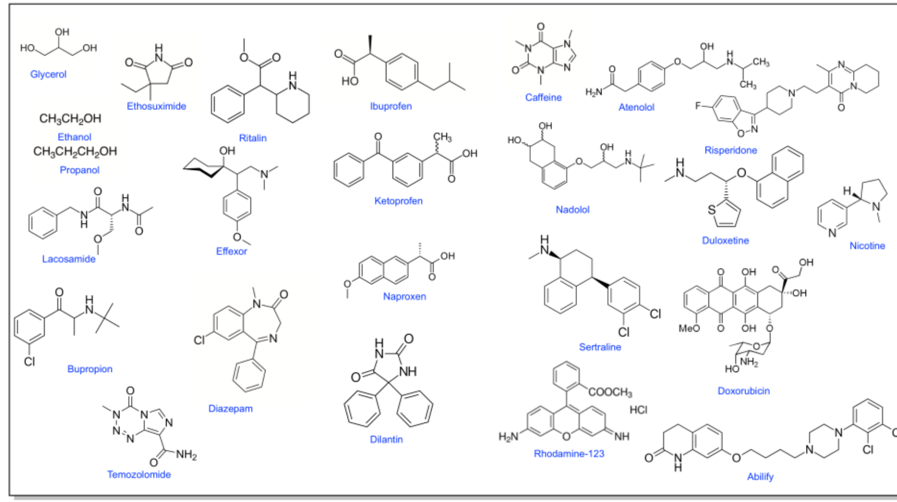

Experimental benchmark data (*N* = 24)

Molecule	MW (g mol^{-1})	H_{donor}	H_{accept}	Log P	DP (debye)	P_{app} (cm s^{-1})	P_{app} Reference	Cell line (2D) or method (3D)
Glycerol	92.09	3	3	-1.8	2.62	9.50×10^{-6}	[87] [Shah 1989]	BMEC
Temozolomide	194.1	1	5	0.4	6.10	1.86×10^{-6}	[88] [Avdeef 2012]	Brain perf (3D)
Caffeine	194.2	0	3	-0.07	3.64	2.10×10^{-5}	IH	MDCK
Ethanol	46.1	1	1	-0.31	1.69	1.10×10^{-3}	[53] [Brahm 1983]	RBC
Propanol	60.1	1	1	0.05	1.68	3.30×10^{-3}	[53] [Brahm 1983]	RBC
Doxorubicin	543.5	6	12	1.27	9.12	1.00×10^{-7}	[89] [Hellinger 2012]	Caco-2 / MDCK
Ethosuximide	141.2	1	2	0.38	1.72	9.00×10^{-6}	[90] [Summerfield 2007]	MDCK
Atenolol	266.3	3	4	0.16	5.00	1.30×10^{-6}	[91] [Adson 1995]	Caco-2
Diazepam	284.7	0	2	2.82	2.65	4.60×10^{-5}	[90] [Summerfield 2007]	MDCK
Nadolol	309.4	4	5	0.81	5.10	3.30×10^{-7}	[92] [Yamashita 2000]	Caco-2
Lacosamide	250.3	2	3	0.73	1.90	1.60×10^{-5}	[93] [Zhang 2013]	Caco-2
Risperdal	410.4	0	6	3.49	5.45	3.00×10^{-5}	[90] [Summerfield 2007]	MDCK
Rhodamine123	380.8	2	5	1.06	6.11	0.80×10^{-7}	[94] [Katt 2019]	iPSC
Dilantin	252.3	2	2	2.47	2.73	2.70×10^{-5}	[90] [Summerfield 2007]	MDCK
Ketoprofen	254.3	1	3	3.12	4.44	8.00×10^{-5}	[95] [Sun 2002]	Caco-2
Naproxen	230.3	1	3	3.18	2.25	3.90×10^{-5}	[96] [Pade 1998]	Caco-2
Nicotine	162.2	0	2	1.17	1.64	1.78×10^{-4}	[97] [Garberg 2005]	Caco-2 / MDCK
Ibuprofen	206.3	1	2	3.97	1.64	2.70×10^{-5}	IH	MDCK
Effexor	277.0	1	3	3.2	3.33	6.00×10^{-5}	[89] [Hellinger 2012]	Caco-2 / MDCK
Ritalin	233.1	1	3	2.25	2.13	2.47×10^{-5}	[98] [Yang 2016]	MDCK
Sertraline	306.2	1	1	5.10	3.86	2.1×10^{-6}	[90] [Summerfield 2007]	MDCK
Duloxetine	297.4	1	3	4.00	2.18	1.66×10^{-5}	[89] [Hellinger 2012]	Caco-2 / MDCK
Bupropion	239.7	2	4	3.60	1.15	4.75×10^{-5}	[90] [Summerfield 2007]	MDCK

Parametrising the BBB workflow

Permeability invariant to simulation box choices (should be!)

$$P_{sim} = \frac{r}{2AC}$$

#: number of permeation events
k: rate constant (ns^{-1})
r: molar rate constant ($mol\ ns^{-1}$)
A: Area of lipid patch (nm^2)
C: Concentration solute ($mol\ dm^{-3}$)
P: permeability ($cm\ s^{-1}$)

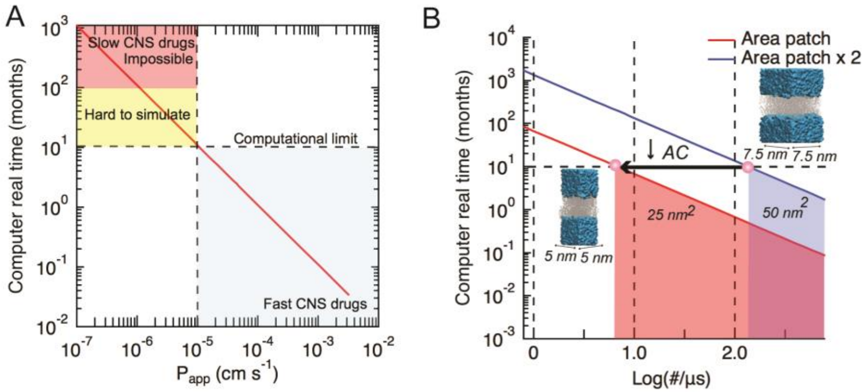

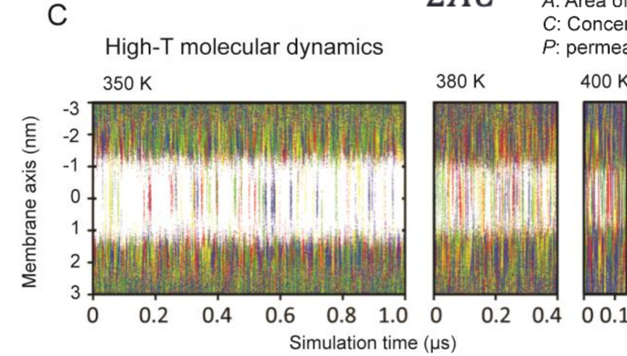

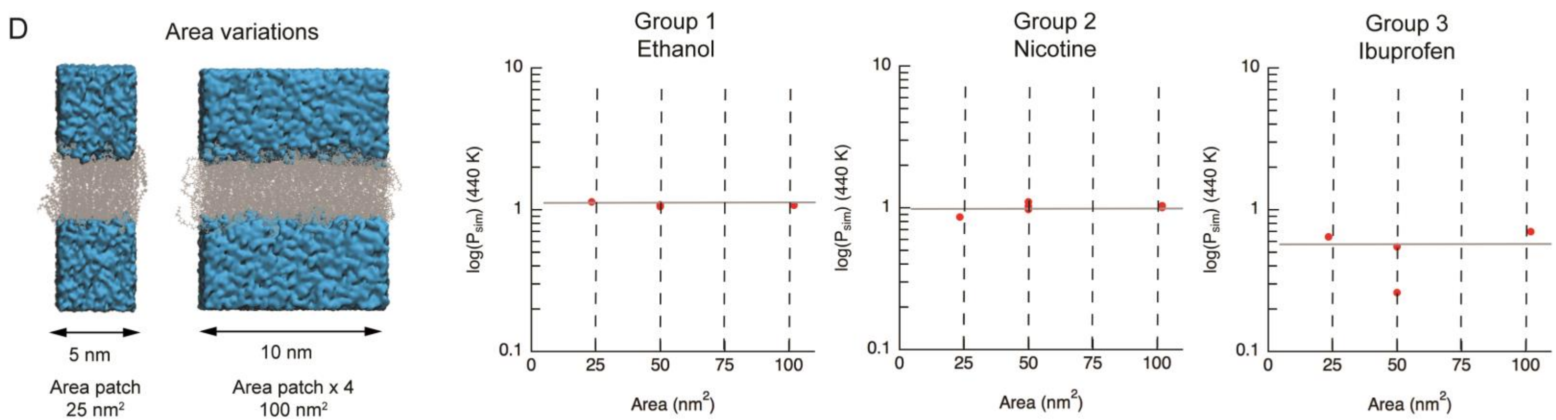

Permeability consistent with box size and volume

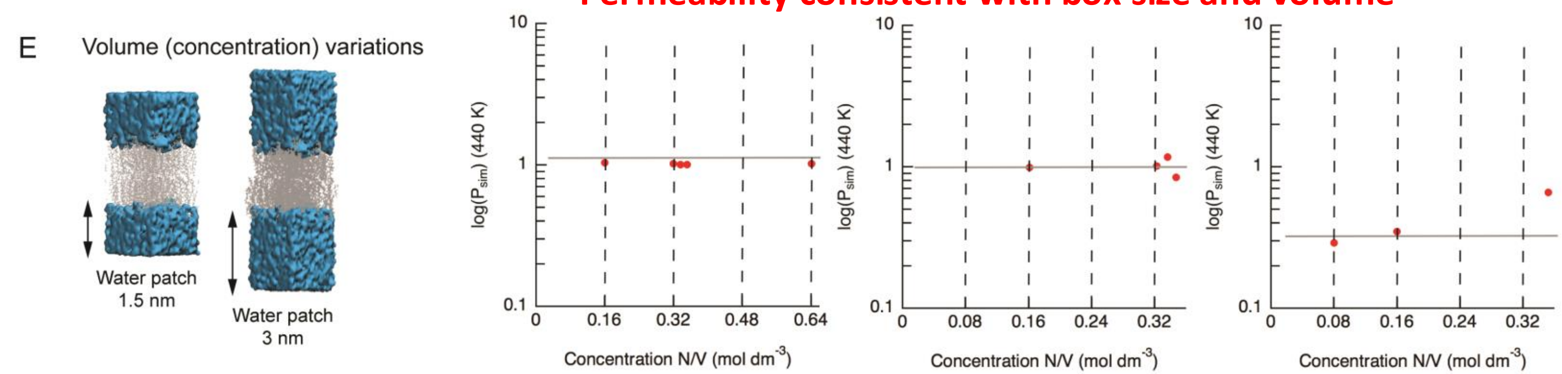

Representative CNS drug library

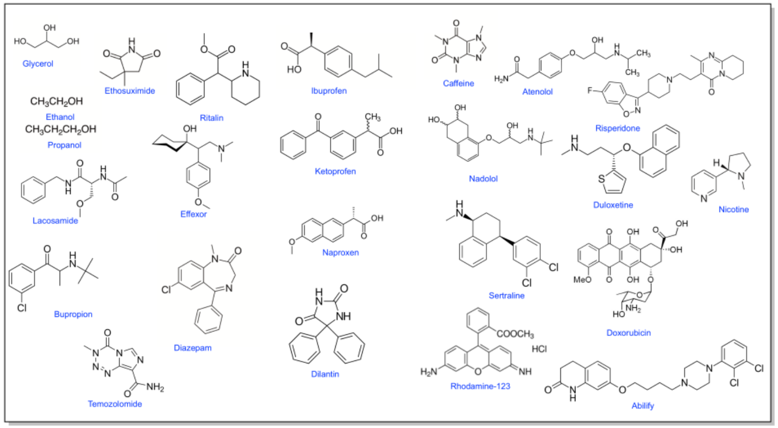

Barrier topologies

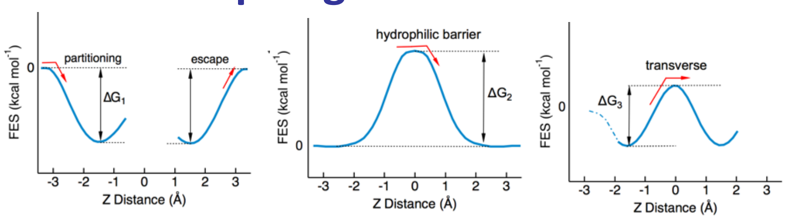

- We introduce terminology to classify distinct types of free-energy barriers
- ΔG_1 : an escape free-energy barrier associated with partitioning into the membrane center
- ΔG_2 : barrier associated with polar, hydrophilic molecules crossing the BBB
- ΔG_3 : barrier from a double-well, transverse free-energy surface

Free-energies of an *N* = 24 compound library clustered according to barrier heights

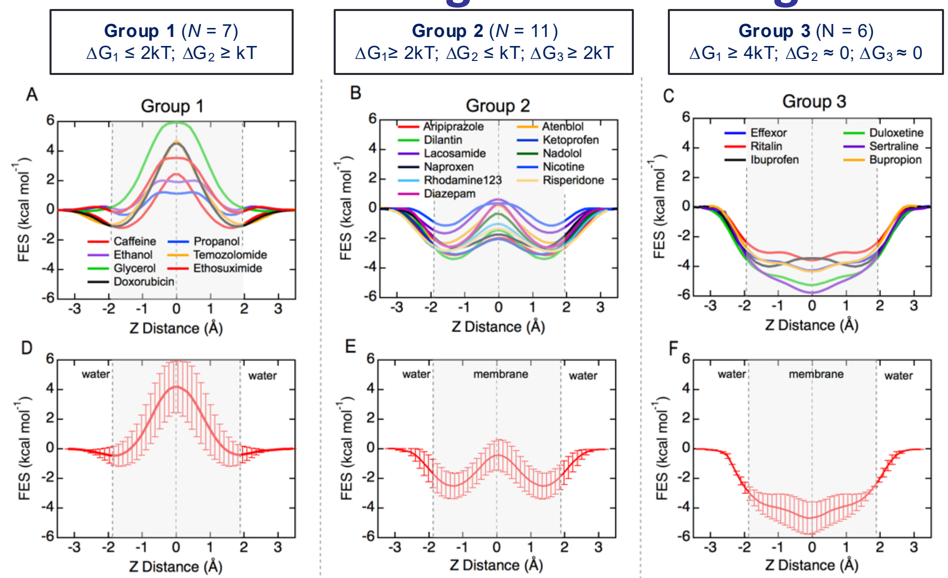

Ethanol Nicotine Ibuprofen

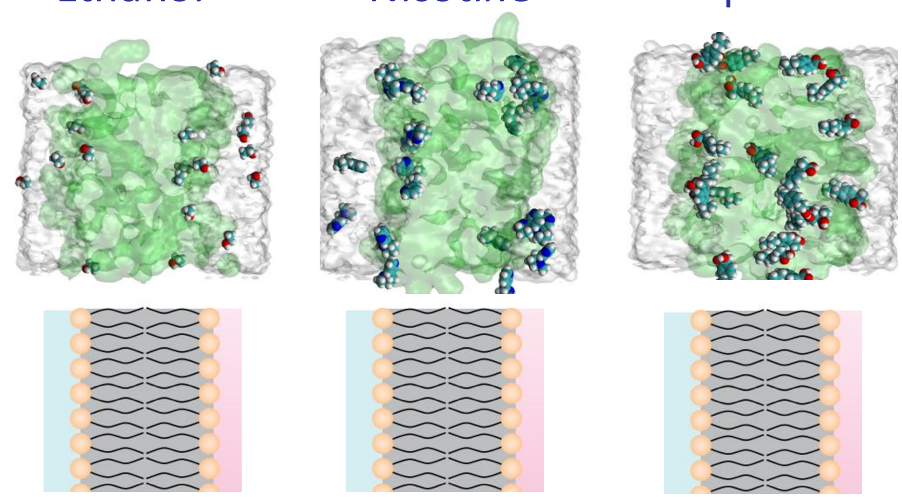

C. Jorgensen, M. B. Ulmschneider, P. C. Searson, *ACS Omega*, **2022**

Validating that the groups are statistically significant

Input parameters (chemical)

- **Log*P*:** n-octanol and water partition coefficient
- **MW**: Molecular weight (g)
- **PSA**: Polar surface area
- **DP:** Total dipole moment (Debye)
- **HB donors**: h-bond donors in a molecule
- **HB acceptor**: h-bond acceptors in a molecule
- **Six membered rings**: Number of 6-memb rings
- **Five membered rings**: Number of 5-memb rings

Input parameters (simulation)

- **Residence time**: Average time inside bilayer
- **Attempt time**: Average time inside bilayer for failed trans
- **# Succesful transitions:** Number of transitions
- **# Attempts:** Number of failed transitions
- **k Rate constant:** # Transitions / simulation time (1/ns)
- **Permeability**: (cm/s) at 440 K
- **ΔG_1**: Lipophilic escape barrier
- **ΔG_2**: Polar drug crossing barrier
- **ΔG_3**: Transversal crossing barrier

Free-energies of an *N* = 24 compound library clustered according to barrier heights

Group 1 (*N* = 7)	**Group 2** (*N* = 11)	**Group 3** (N = 6)
$\Delta G_1 \leq 2kT$; $\Delta G_2 \geq kT$	$\Delta G_1 \geq 2kT$; $\Delta G_2 \leq kT$; $\Delta G_3 \geq 2kT$	$\Delta G_1 \geq 4kT$; $\Delta G_2 \approx 0$; $\Delta G_3 \approx 0$

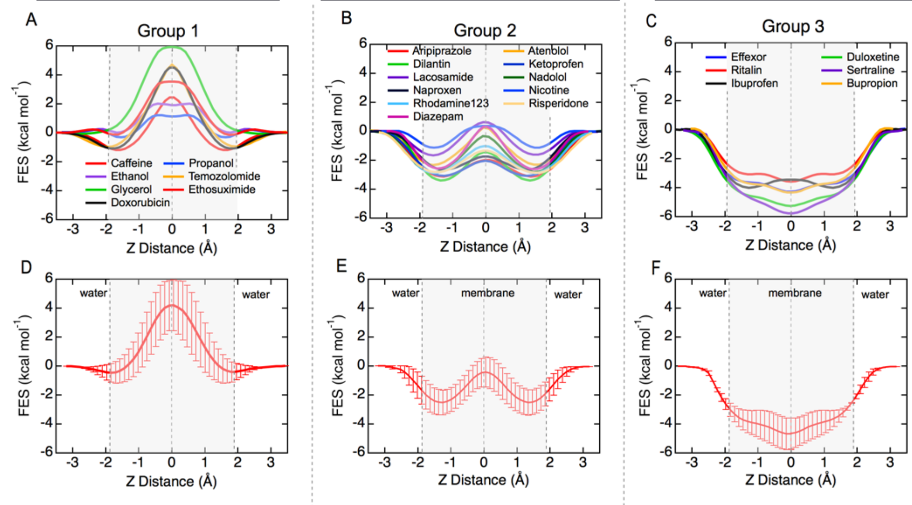

Advantage of workflow: ~ 1 day on a single NVIDIA GPU → possible to screen ~100 compounds per month for a typical cluster

Parameter output

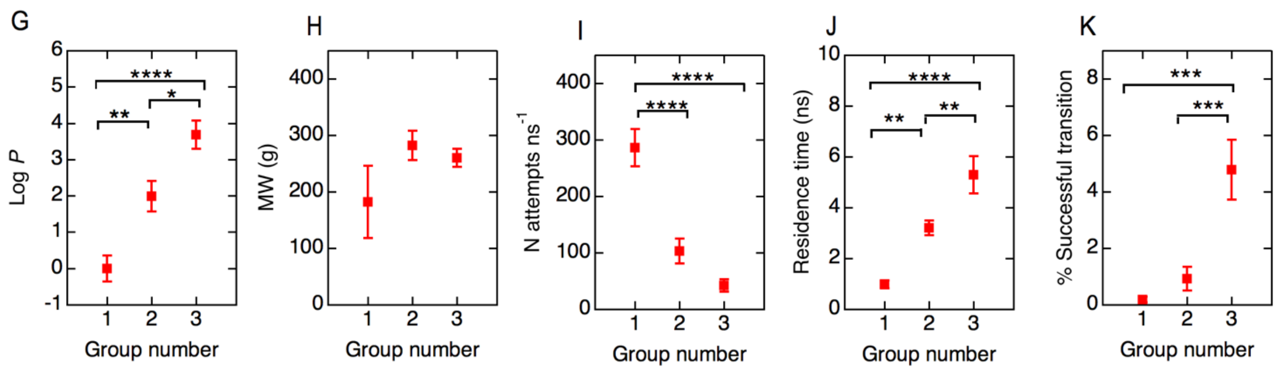

Take-home findings

- Log*P* discretizes across
- the three groups
- MW is not a good descriptor
- (as per Lipinski's rule) for CNS penetration

The big picture: BBB permeability models

Experimental permeability

- **Not generally routine**
- Requires either *in vitro* proxy assays such as Caco-2 or PAMPA for BBB permeation. Sometime even from red blood cells (not ideal)
- In-house BBB model permeability with fluorescence tracking (JHU)

In silico permeability

- **Not routine for the BBB**
- Can use unbiased simulations for drugs with $P_{app} > 10^{-4}$ cm/s.
- For $P_{app} < 10^{-5}$ cm/s we need enhanced sampling techniques as unbiased MD takes between **10^2-10^3 months** on a single GPU.

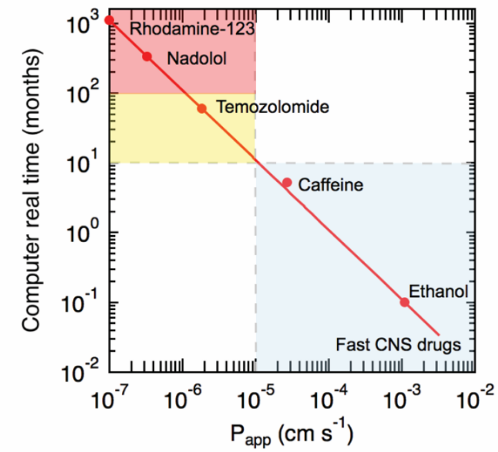

Proposed development: Enhanced sampling approaches for BBB permeability

1. Kramers-based Arrhenius model

Arrhenius extrapolation to 310 K with a correction in non-linear regime. Not routine.

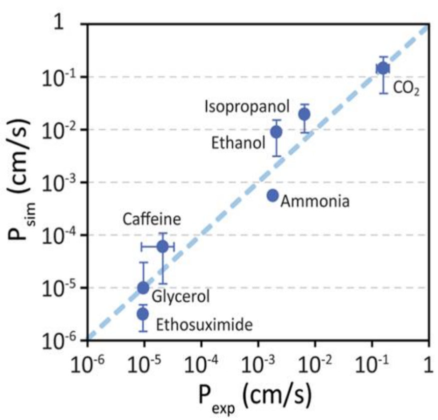

Wang *et al. Sci. Rep.*, **2019**

2. Regression based models

Regression with high-T data. Accuracy to ~1-~2 OM on one GPU. Routine ranking of >10^1 molecules is now routine

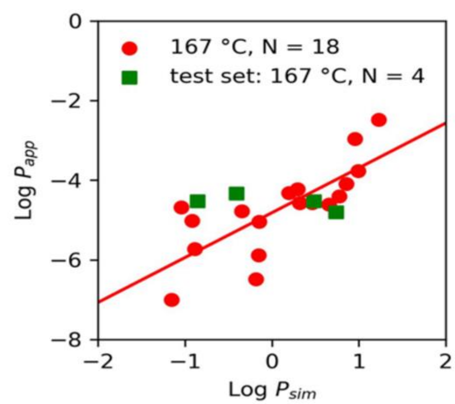

Jorgensen *et al. JCAMD*, **2023**
Jorgensen *et al*, *ACS Omega*, **2022**

3. Permeability via the Green-Kubo equations with steered MD

$$\frac{1}{P} = \int_{-d}^{d} \frac{\exp\left(\beta \Delta G(z)\right)}{D_z(z)} dz$$

$$D_z(z) = \frac{(RT)^2}{\int_0^\infty dt \left\langle \Delta F_z(z,t) \Delta F_z(z,0) \right\rangle}$$

Jorgensen *et al.* *JCIM*, **2025**

Ethanol permeation across the BBB

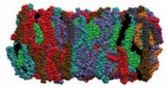

Ethanol: PMF

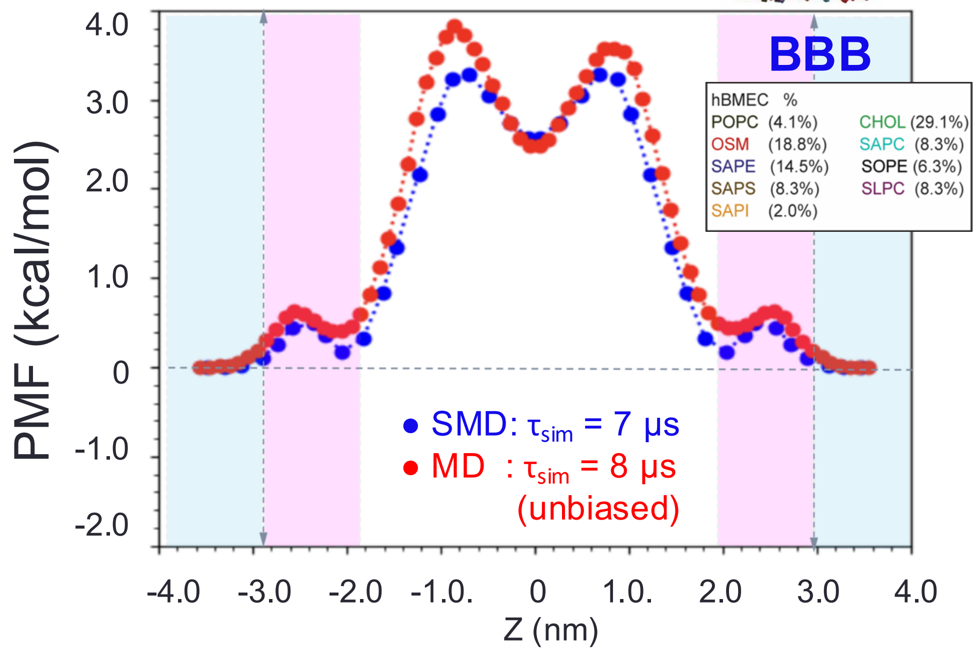

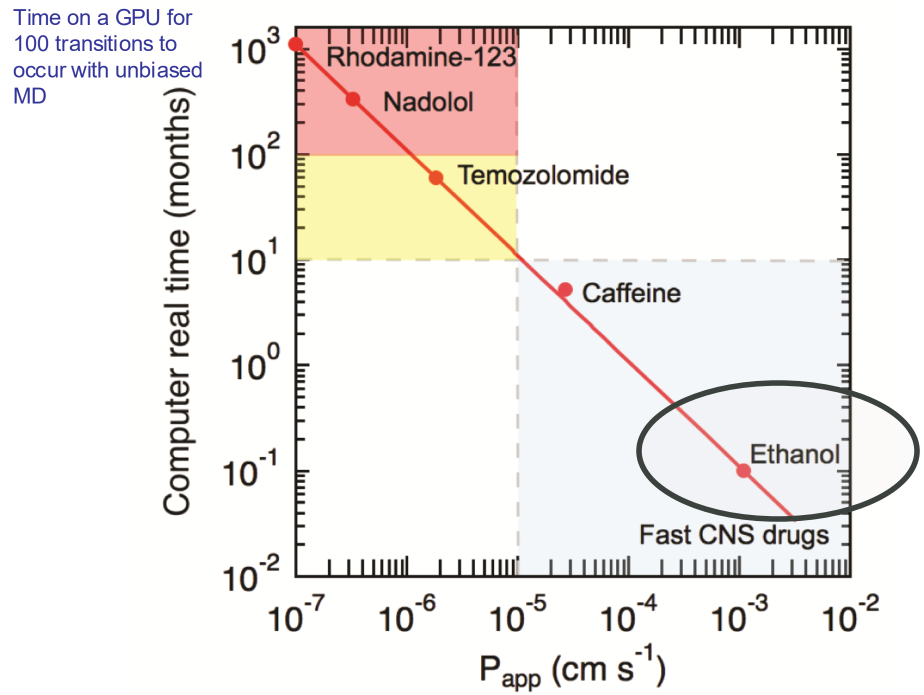

Pure POPC bilayer thickness: ~3.75 nm
Mammalian bilayer thickness: ~4.70 nm

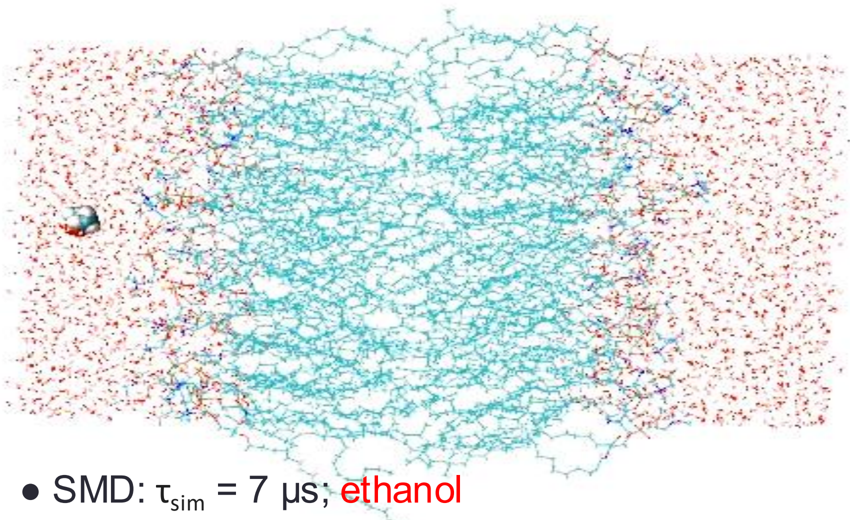

● SMD: τ_{sim} = 7 μs; ethanol

Convergence

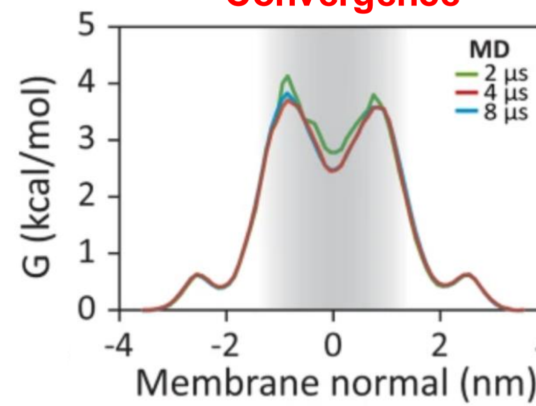

SMD data unpublished
Unbiased MD from Wang *et al.* *Sci. Rep.*, **2019**

Ethanol permeation across the BBB

Ethanol: PMF

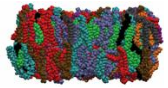

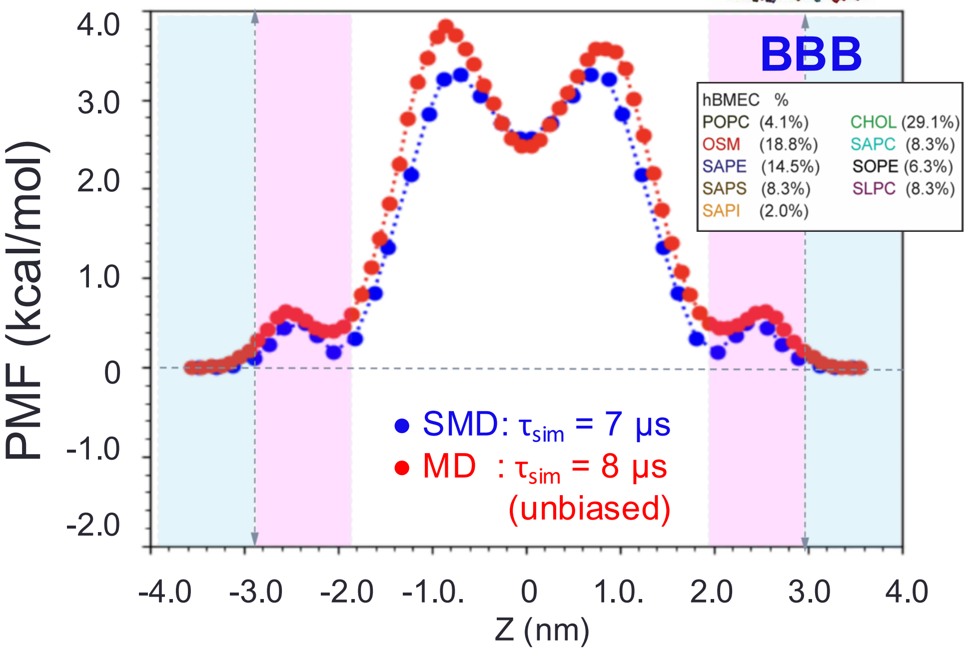

Comer, Schulten, Chipot, *JCTC*, 2017, 13

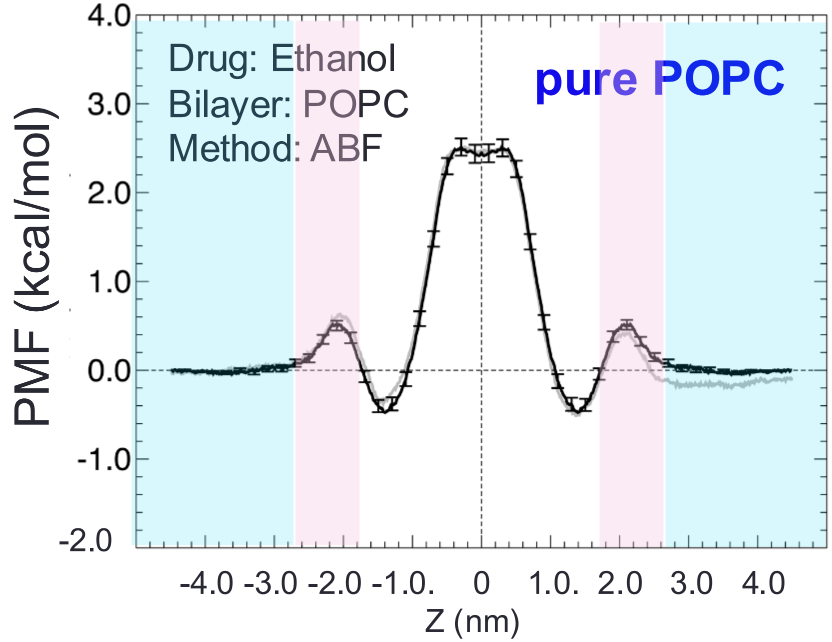

Pure POPC bilayer thickness: ~3.75 nm
Mammalian bilayer thickness: ~4.70 nm

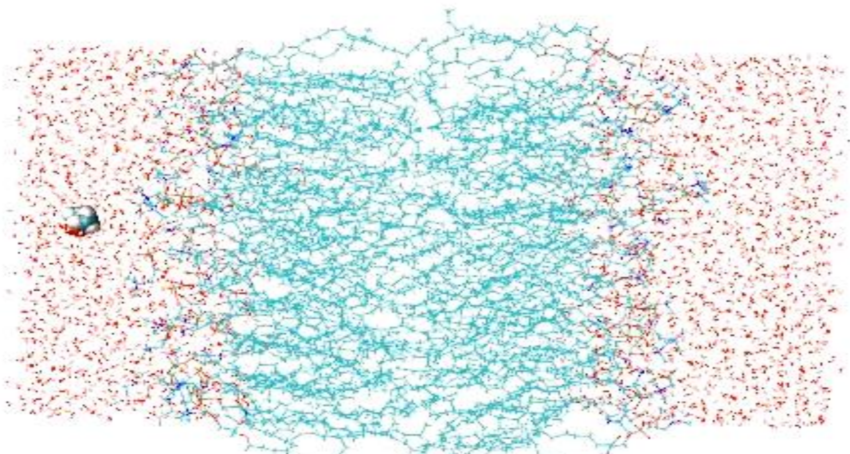

● SMD: τ_{sim} = 7 µs; ethanol

Convergence

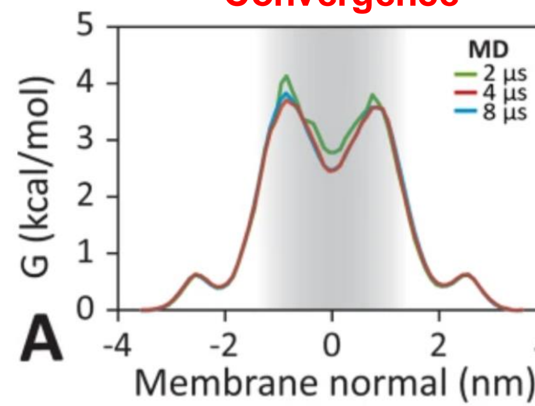

SMD data unpublished

Unbiased MD from Wang *et al. Sci. Rep.*, **2019**

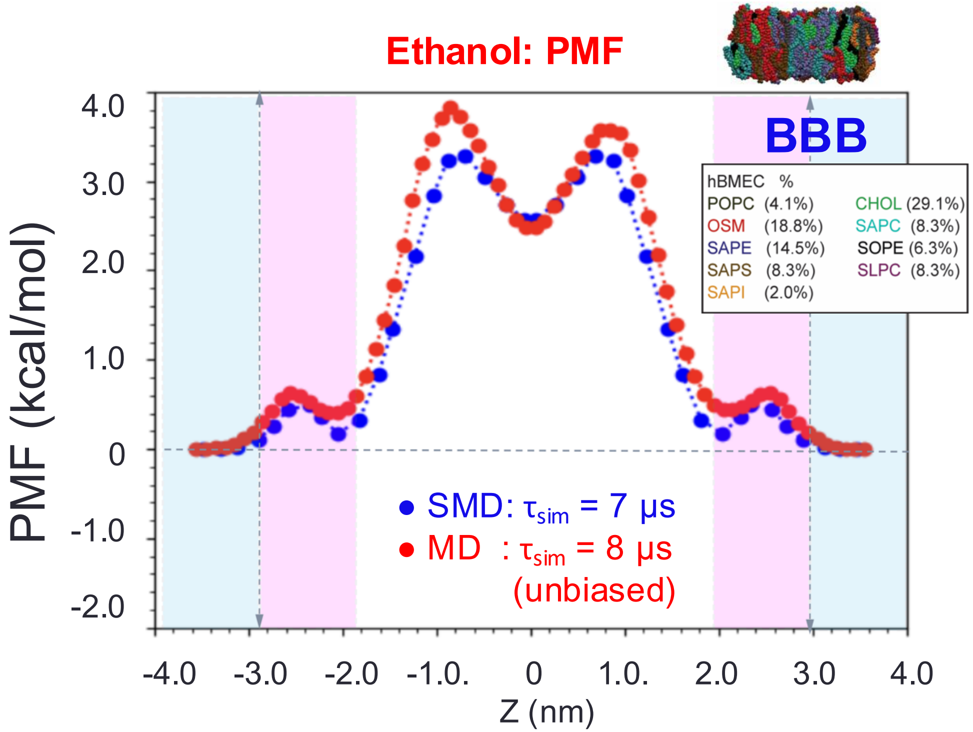

Comer, Schulten, Chipot, *JCTC*, 2017, 13

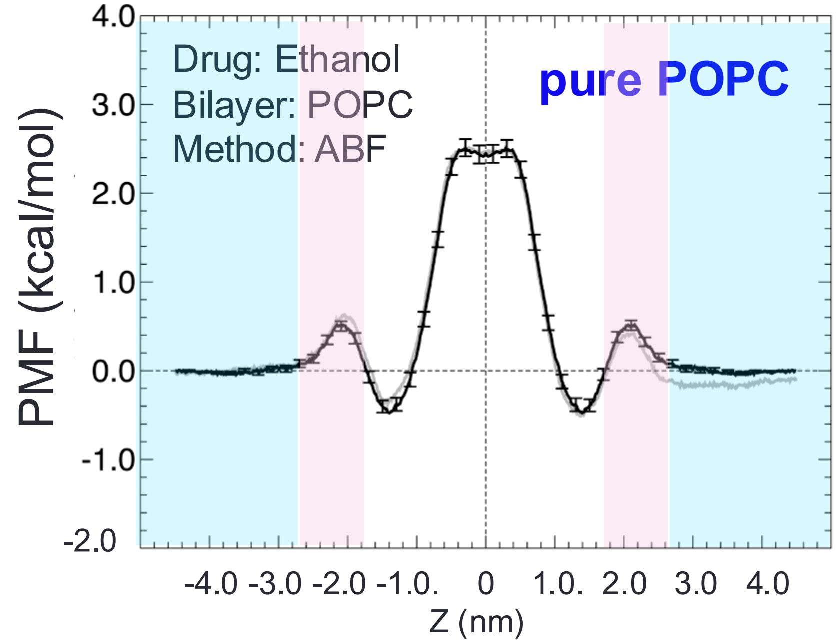

Pure POPC bilayer thickness: ~3.7 nm [1] to ~3.8 nm [2, 3, 5]
Mammalian bilayer thickness: ~4.70 nm [2]
BBB bilayer thickness: ~4.75 nm [6]

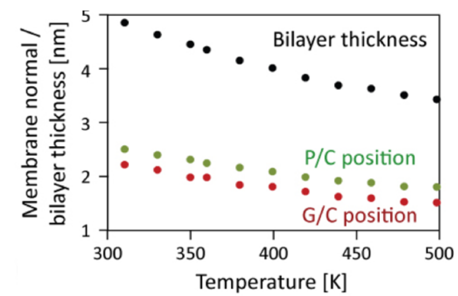

The mammalian lipid bilayer reaches maximal bilayer thickness due to the condensation effect by the predominance of cholesterol [4]

[1] Gullingsrud, J., Schulten, K., *Biophysical journal*, **2004**, *86* (6)
[2] Kucerka, N., Tristram-Nagle, S., Nagle, J.F., *J Membr Biol,* **2005,** 208 (3)
[3] Skjevik, A., Madej, B.D., Dickson C.J., Teigen K., Walker R.C., Gould I.R. *Chem Commun*, **2015,** 51(21)
[4] Shahane, G., *et al. Journal of molecular modeling*, **2019**, *25*
[5] Pöhnl, M., Trollmann, M. F., & Böckmann, R. A. *Nat. Comms*, **2023**, 14(1)
[6] Y. Wang, E. Gallagher, C. Jorgensen, E. P. Troendle, D. Hu, P. C. Searson, M. B. Ulmschneider, *Sci. Rep.,* **2019,** 9

- 3 SMD simulations
- τ_{sim} = 7 μs each

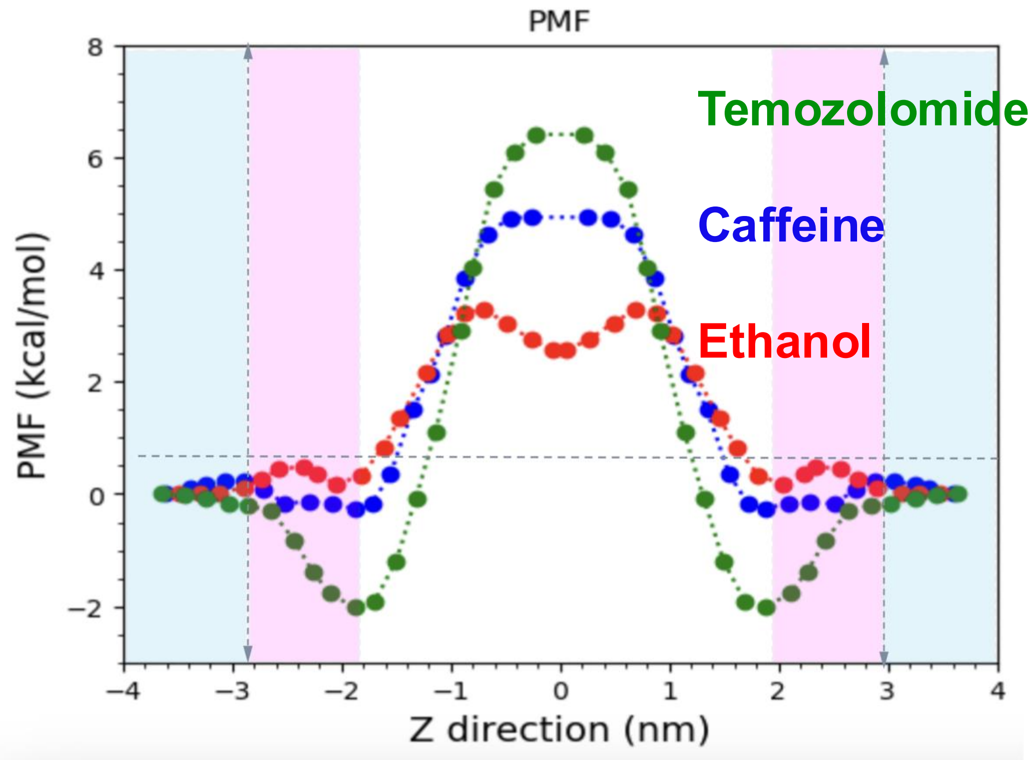

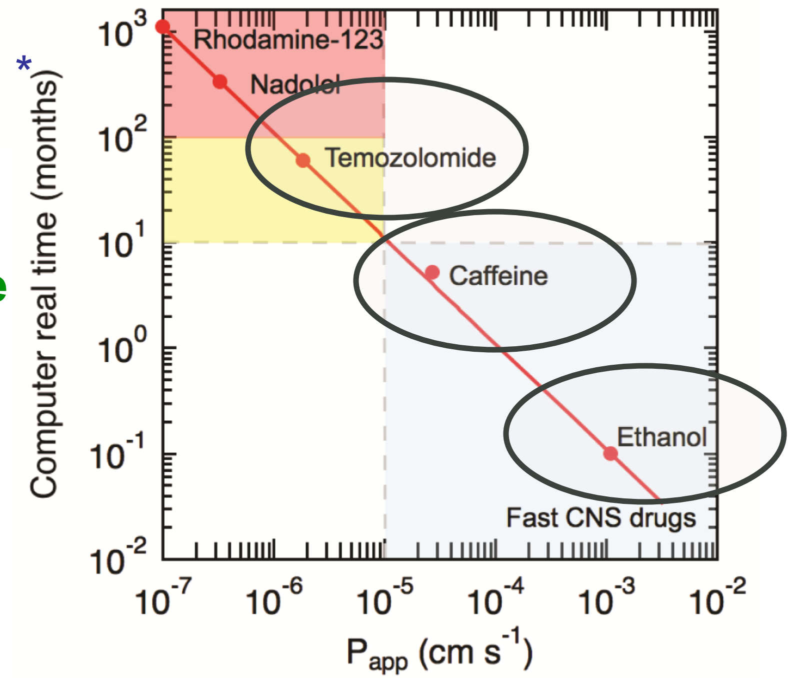

*Time on a GPU for 100 transitions to occur with unbiased MD

In press

Temozolomide
LogP_{ow} = -0.21

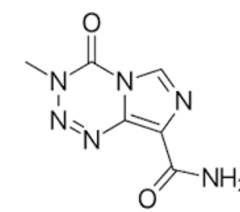

Caffeine
LogP_{ow} = -0.07

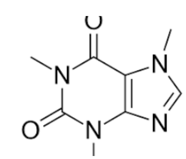

Ethanol
LogP_{ow} = -0.31

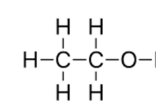

- 3 SMD simulations
- τ_{sim} = 7 µs each

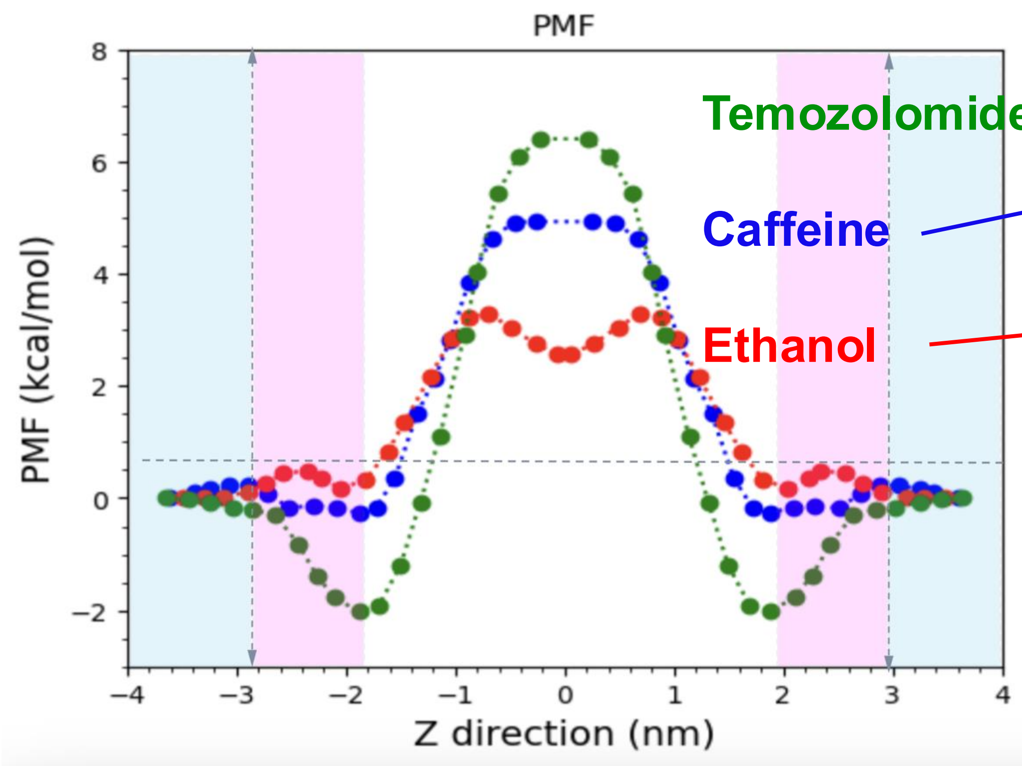

Temozolomide

Caffeine

Ethanol

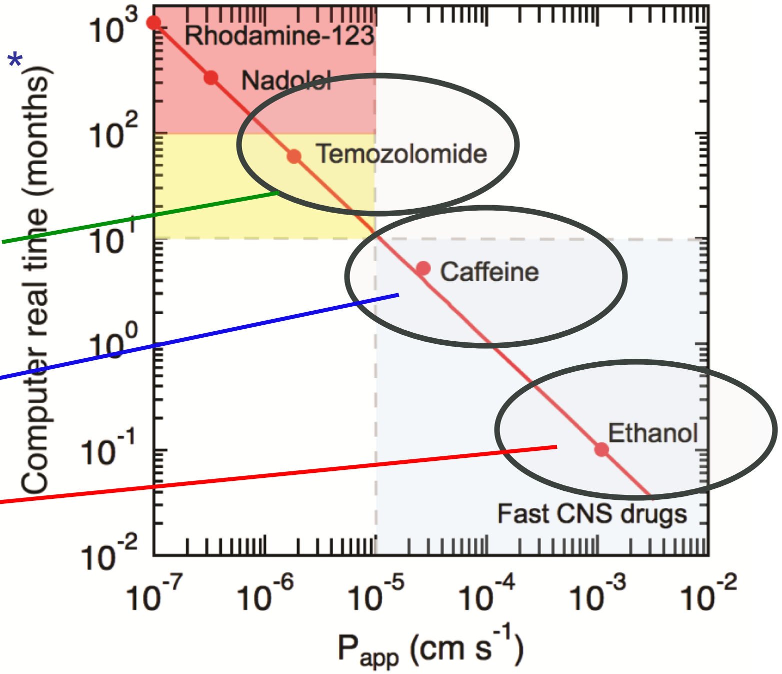

*Time on a GPU for 100 transitions to occur with unbiased MD

Temozolomide
$\mathrm{Log}P_{ow}$ = -0.21

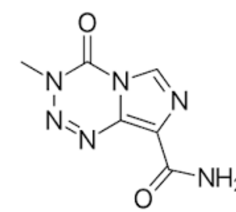

Caffeine
$\mathrm{Log}P_{ow}$ = -0.07

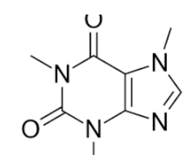

Ethanol
$\mathrm{Log}P_{ow}$ = -0.31

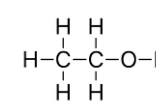

In press

Motivation

- P-glycoprotein is a protective pump that keeps out exogenous chemicals from the brain. It is the leading cause of multidrug resistance to chemotherapeutics crossing the BBB
- P-gp is non-specific (over 300 known substrates). But WHY?

JOHNS HOPKINS UNIVERSITY

Searson

Schiøtt

Computing time

MARCC Maryland Advanced Research Computing Center

Funding: MSCA IF 101023783

MARIE CURIE ACTIONS

AARHUS UNIVERSITY

1. Passive CNS penetration

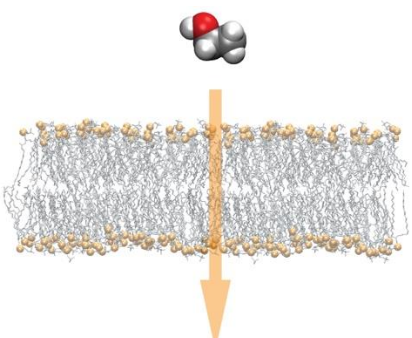

2. Efflux out (drug resistance)

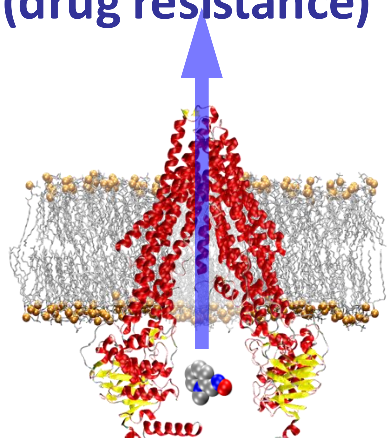

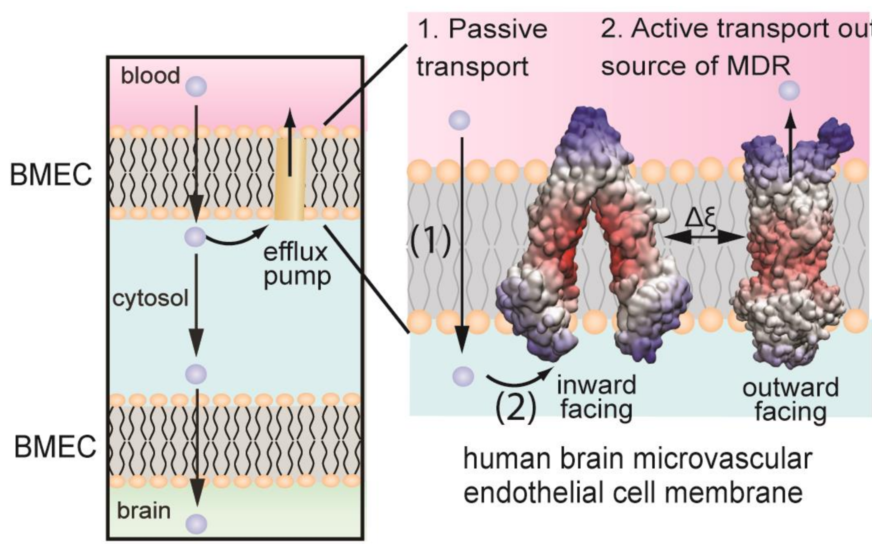

C. Jorgensen, M. B. Ulmscheider, P. C. Searson, *J. Med. Chem.*, **2023**, *66*
C. Jorgensen et al.*JCIM*, **2025**, *65*

How to understand efflux? Build a P-gp model

1. Kinetic model

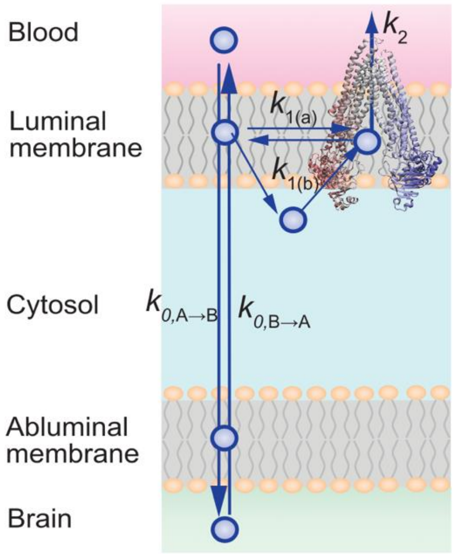

- Understand substrate interaction with P-gp in terms of rate constants k_0, $k_{1(a)}$ and $k_{1(b)}$
- Use simulations to estimate the three *k* values to mathematically **understand** efflux

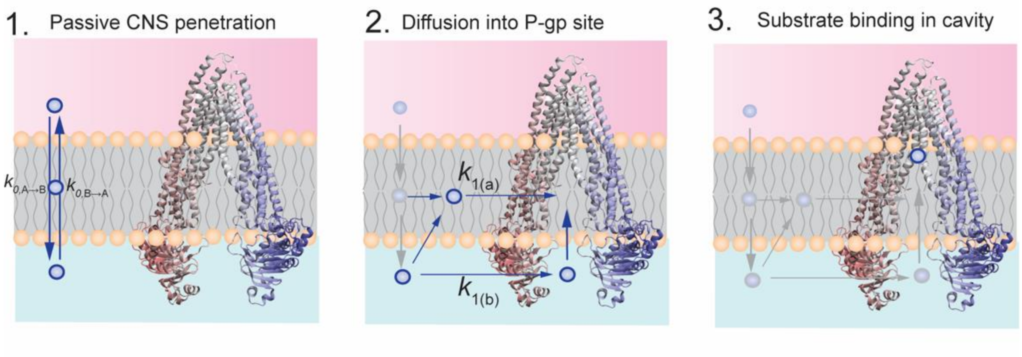

C. Jorgensen, M. B. Ulmscheider, P. C. Searson, *J. Med. Chem.*, **2023**, *66*

How to understand efflux? Build a P-gp model

1. Kinetic model

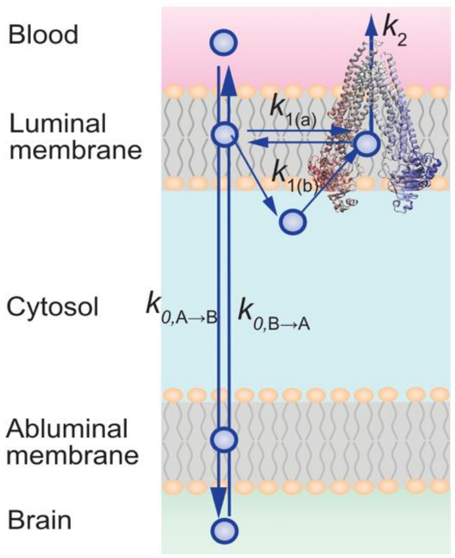

- Understand substrate interaction with P-gp in terms of rate constants k_0, $k_{1(a)}$ and $k_{1(b)}$
- Use simulations to estimate the three k values to mathematically **understand** efflux

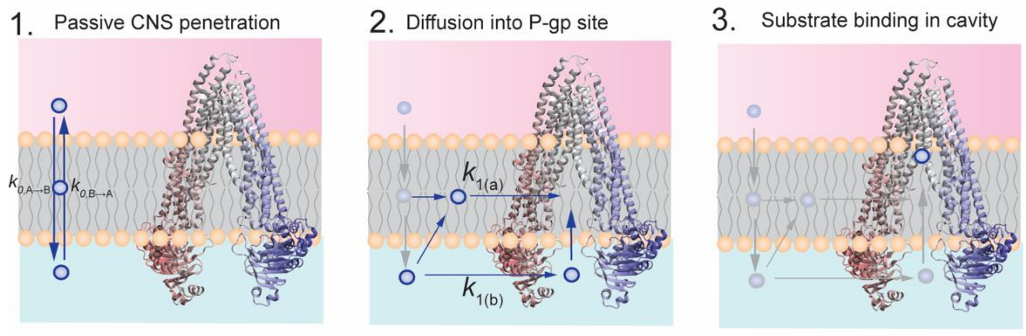

2. Geometric model

- Understand P-gp conformational dynamics

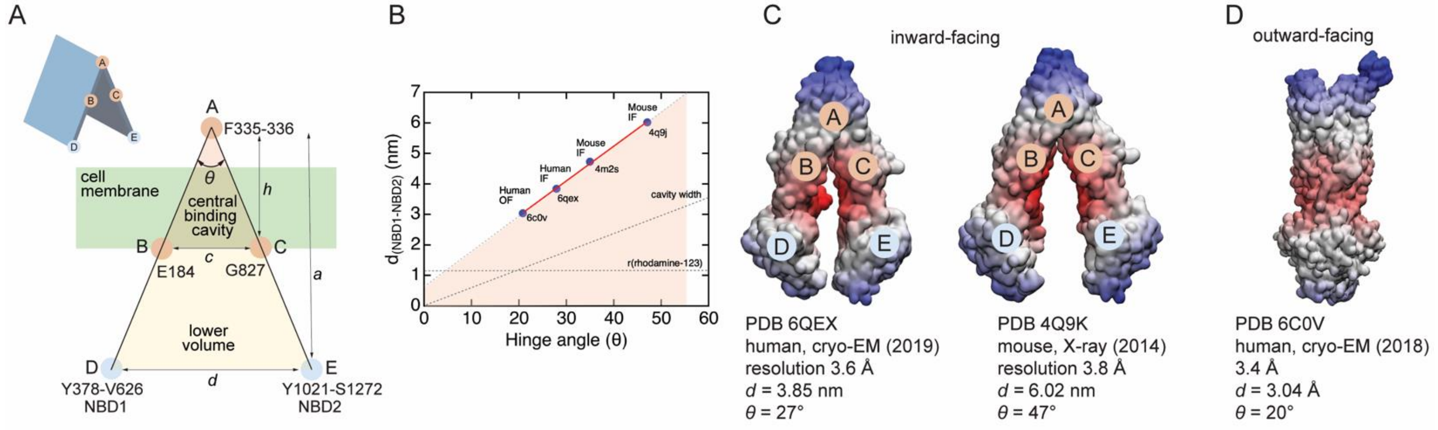

C. Jorgensen, M. B. Ulmscheider, P. C. Searson, *J. Med. Chem.*, **2023**, *66*

How to understand efflux? Build a P-gp model

1. Kinetic model

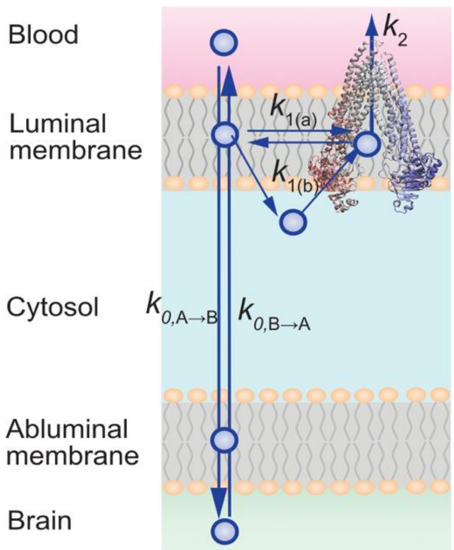

- ➢ Understand substrate interaction with P-gp in terms of rate constants k_0, $k_{1(a)}$ and $k_{1(b)}$
- ➢ Use simulations to estimate the three k values to mathematically **understand** efflux

3. Simulation model

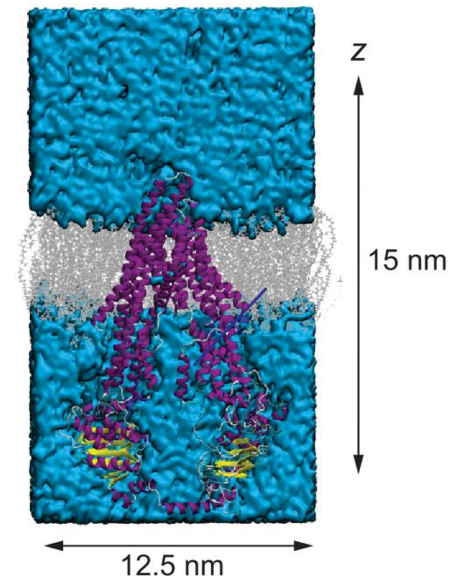

2. Geometric model

- ➢ Understand P-gp conformational

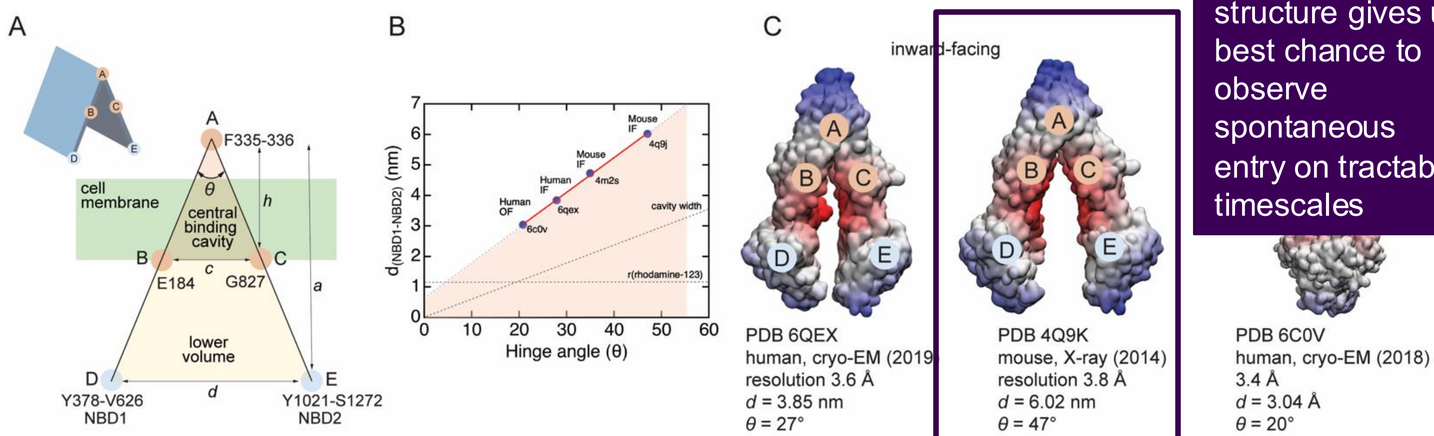

We believe this structure gives us best chance to observe spontaneous entry on tractable timescales

C. Jorgensen, M. B. Ulmscheider, P. C. Searson, *J. Med. Chem.*, **2023**, *66*

Substrates and Inhibitors of P-gp

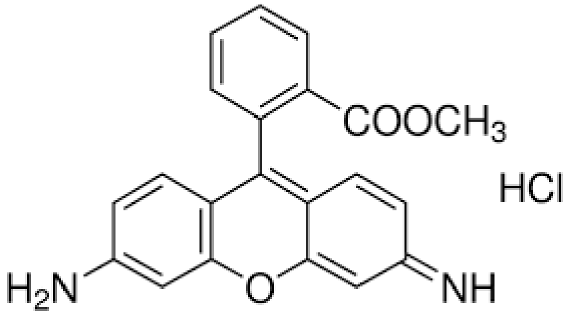

Rhodamine-123

$P_{app} \sim 1 \times 10^{-7}$ cm s^{-1} (slow transport)
Efflux ratio ~5 (i.e. P-gp substrate)

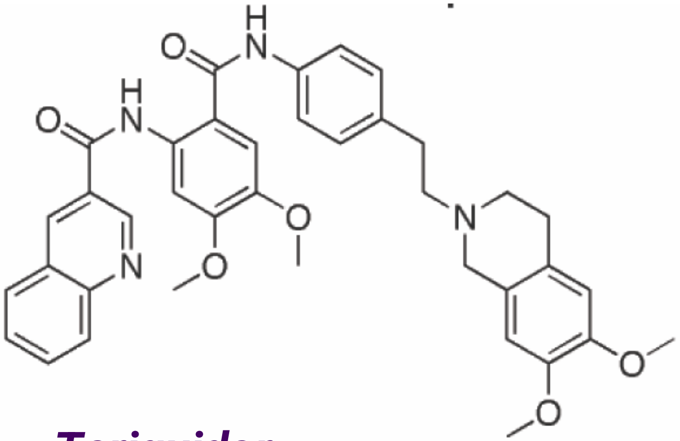

Tariquidar

Potent third-generation inhibitor
k_d = 5.1 nM

- Direct substrate entry into P-gp has **never** been observed experimentally or in a simulation
- 1st gen. inhibitors have been observed crystallographically bound in P-gp central binding cavity but the **mechanism of inhibition** is disputed

Efflux ratio = $P_{b\text{->}a}$ / $P_{a\text{->}b}$

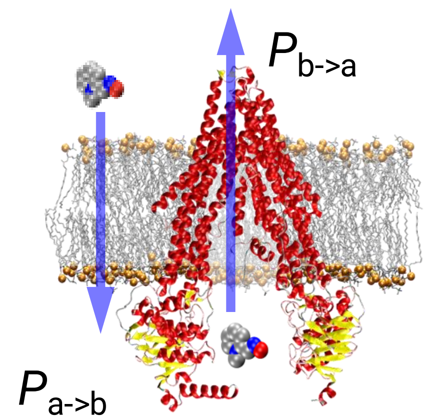

(1) Passive diffusion k_0

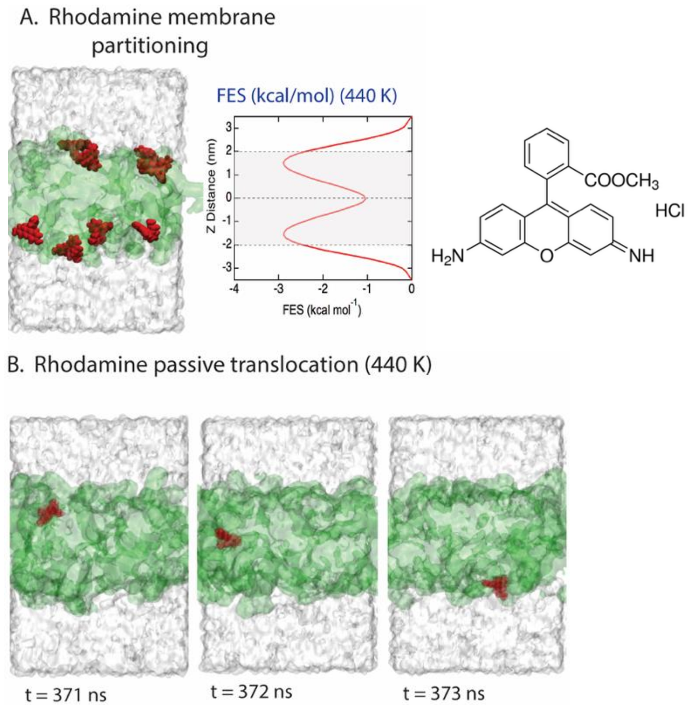

- The free energy surface for partitioning of rhodamine at 440 K has an **energy maximum** at the **hydrophobic core** of the bilayer (***z* = 0.0 nm**) and energy **minima** (with respect to bulk solution) in the polar headgroup regions (***z* = ± 1.7 nm**)
- Consistent with the observation that rhodamine-123 accumulates in mitochondrial membranes.

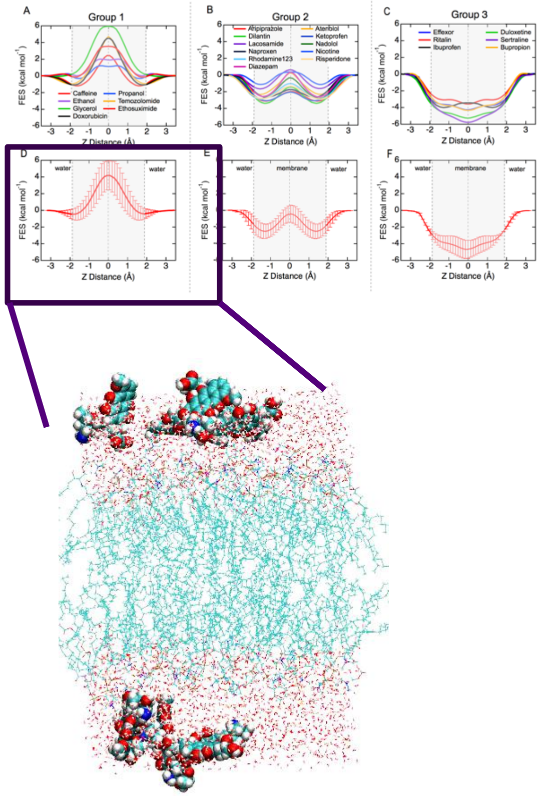

(2) Flooding simulation for k_1 of rhodamine in a P-gp BBB system

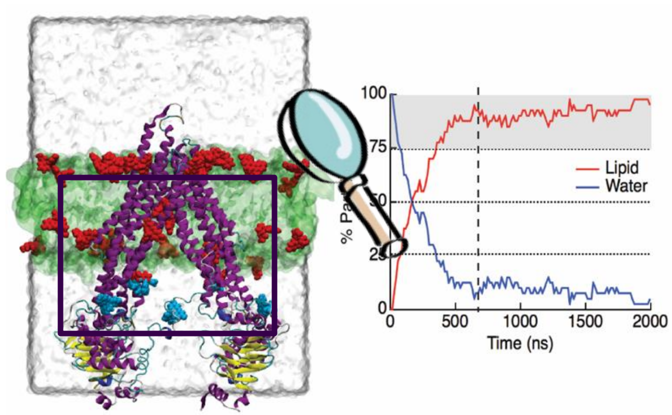

- **80% of rhodamine-123** molecules accumulate in the membrane

Simulation specs

GROMACS 2020
CHARMM-36 ff
2.0 μs simulation
40 rhodamine in box

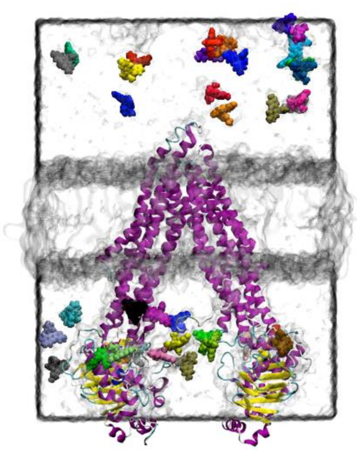

➢ **Substrate entry observed for the first time via simulations**

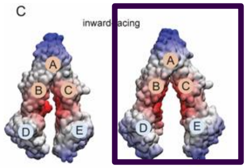

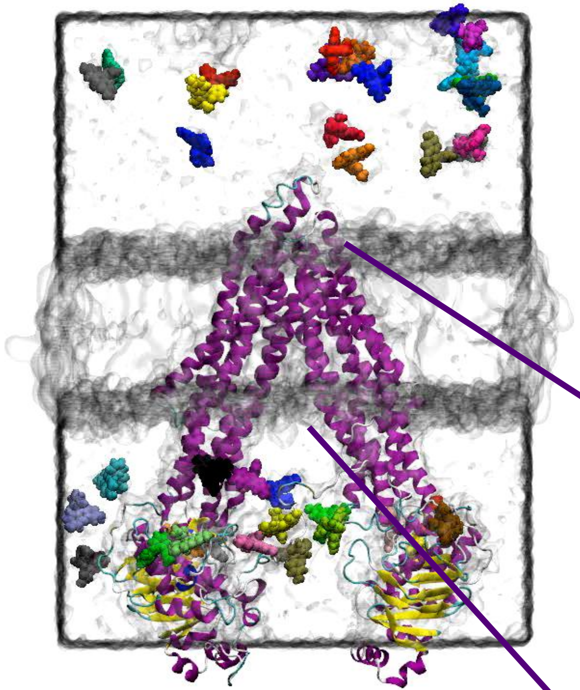

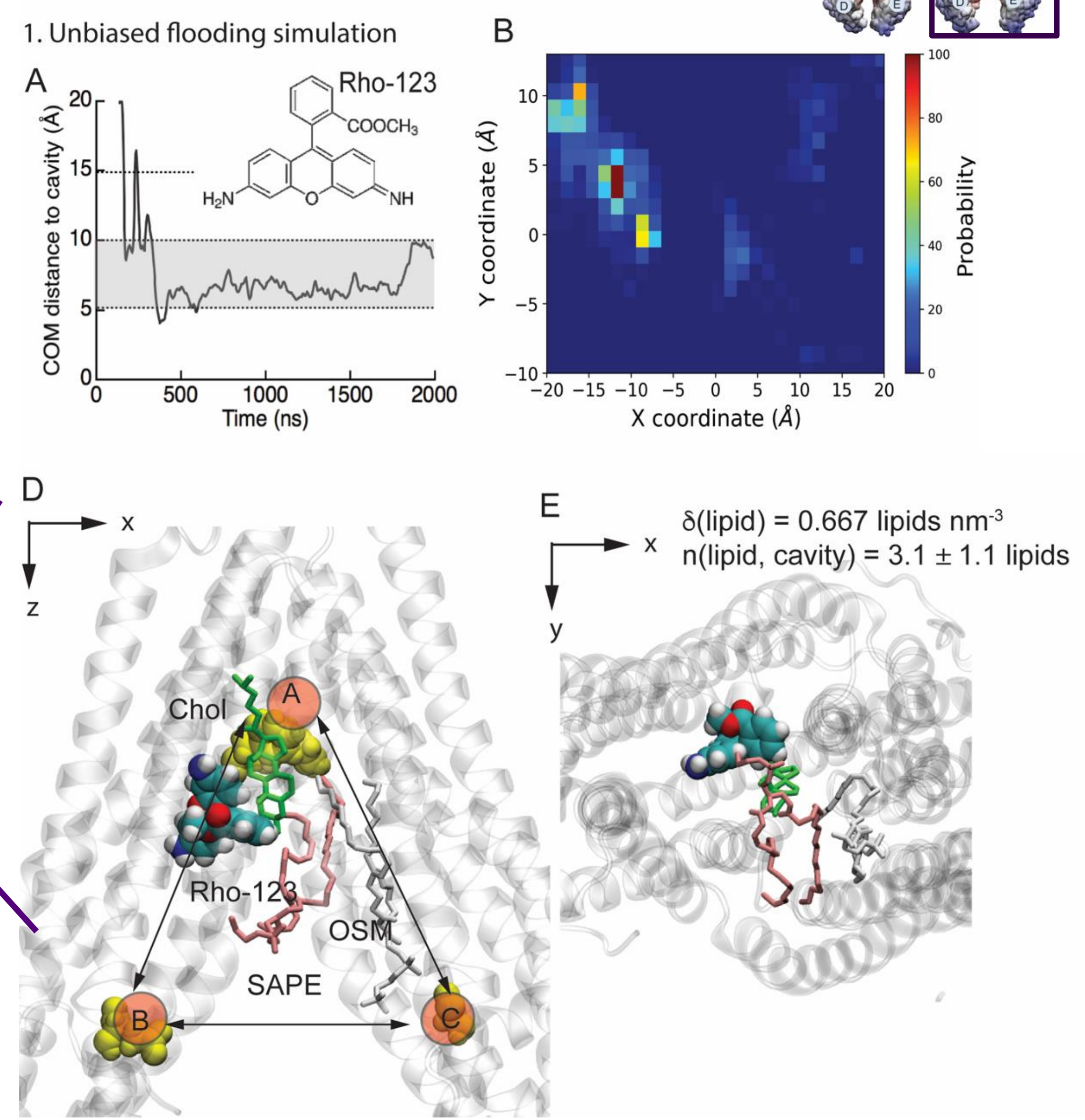

Simulation specs

GROMACS 2020
CHARMM-36 ff
2.0 μs simulation
40 rhodamine in box

C. Jorgensen, M. B. Ulmscheider, P. C. Searson, *J. Med. Chem.*, **2023**, *66*

➢ k_1 estimation: Lateral ($k_{1(a)}$) vs. aqueous ($k_{1(b)}$) pathways

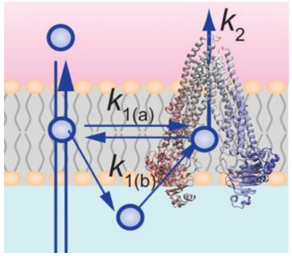

~100 days on a supercomputer

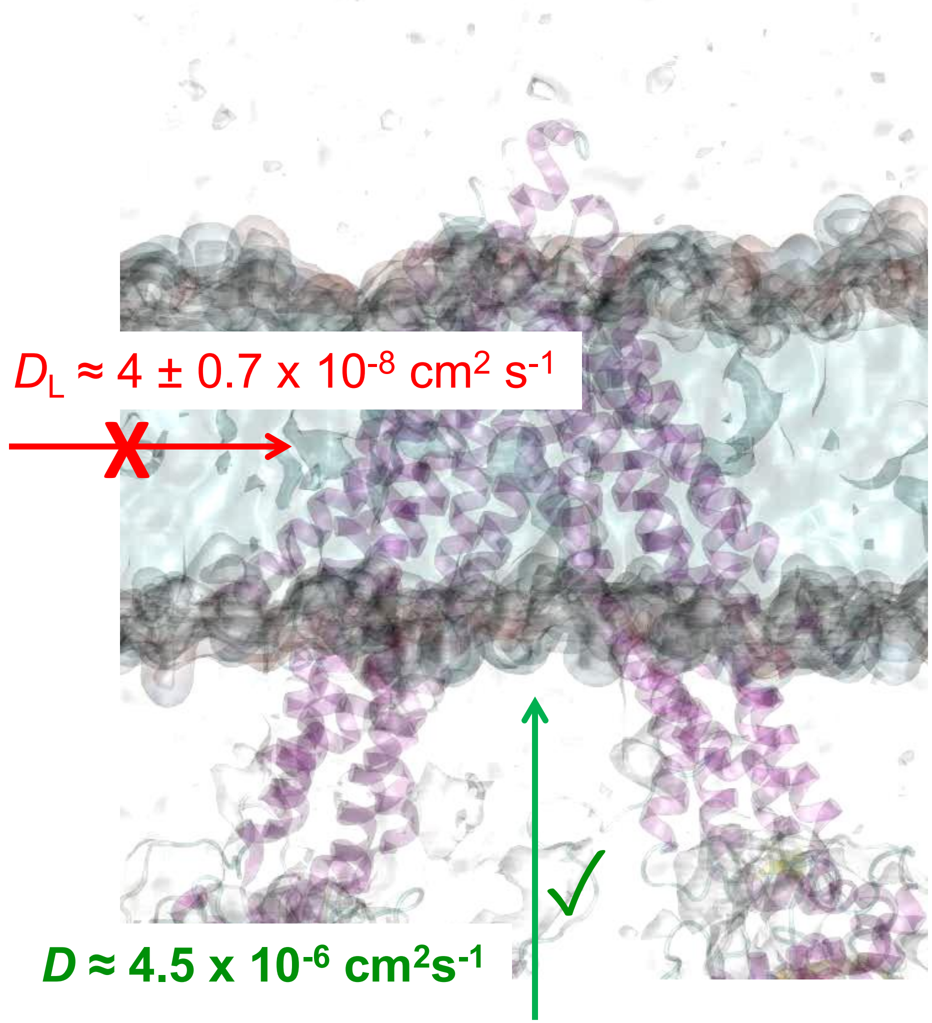

- **Lateral diffusion mechanism $k_{1(a)}$**: Lateral diffusion constant, D_L, of a rhodamine in the minimum free-energy well was estimated from least-squares fit of the mean-square displacement (MSD) as **$D_L \approx 4 \pm 0.7 \times 10^{-8}\ cm^2\ s^{-1}$**

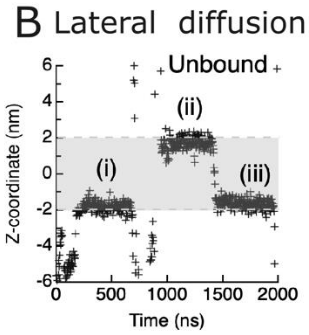

- **Aqueous diffusion mechanism $k_{1(b)}$**: From MSD of rhodamine-123 diffusion in bulk: **$D \approx 4.5 \times 10^{-6}\ cm^2 s^{-1}$**

- Conclusion: Aqueous pathway much more likely. We estimate **only 5.6 %** rhodamine molecules crossing the membrane laterally into the P-gp cavity.

C. Jorgensen, M. B. Ulmscheider, P. C. Searson, *J. Med. Chem.*, **2023**, *66*

Inhibition of P-gp to prevent MDR

Inhibition of P-gp by tariquidar via MD simulation

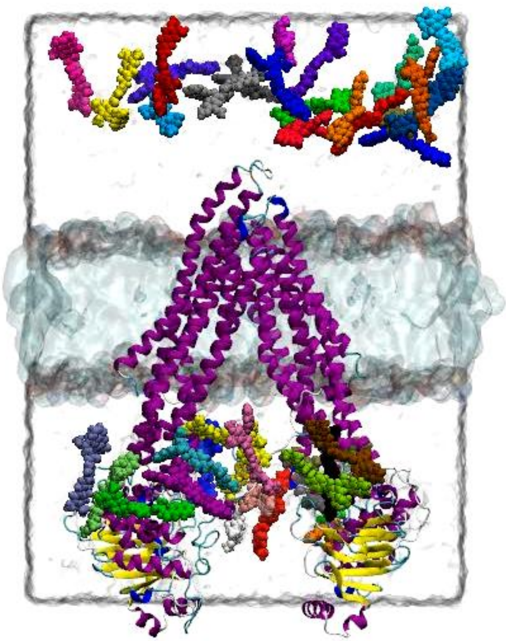

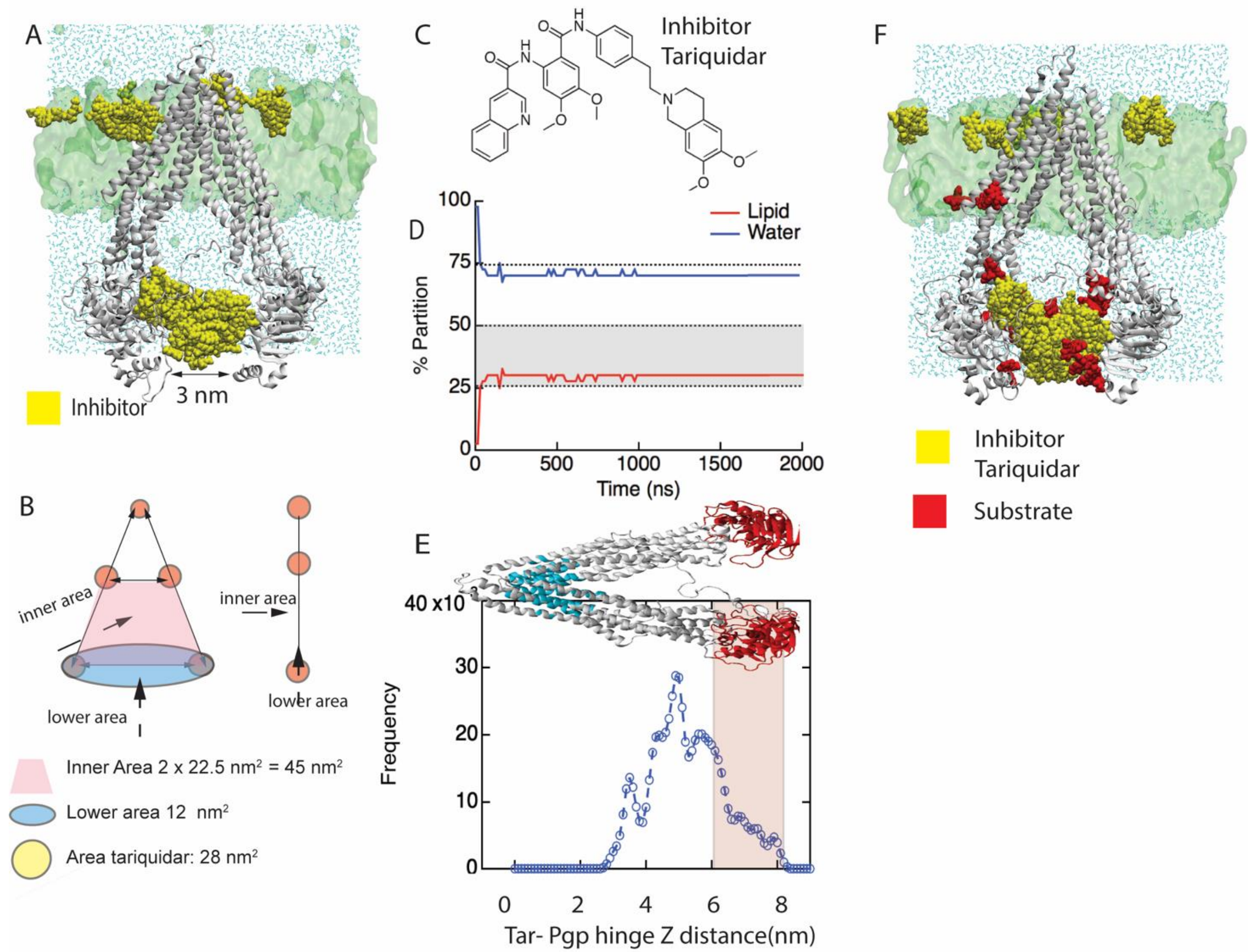

Sim. Specs

GROMACS 2020
CHARMM-36 ff
2.0 μs simulation
40 tariquidar in box

C. Jorgensen, M. B. Ulmscheider, P. C. Searson, *J. Med. Chem.*, **2023**, *66*

Replicates suggest tariquidar aggregation (19 ± 1) is an early stage in the inhibition mechanism

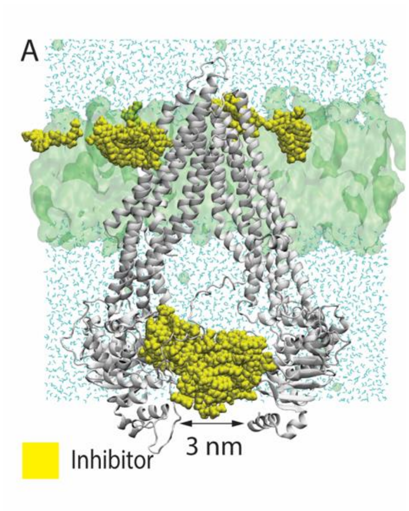

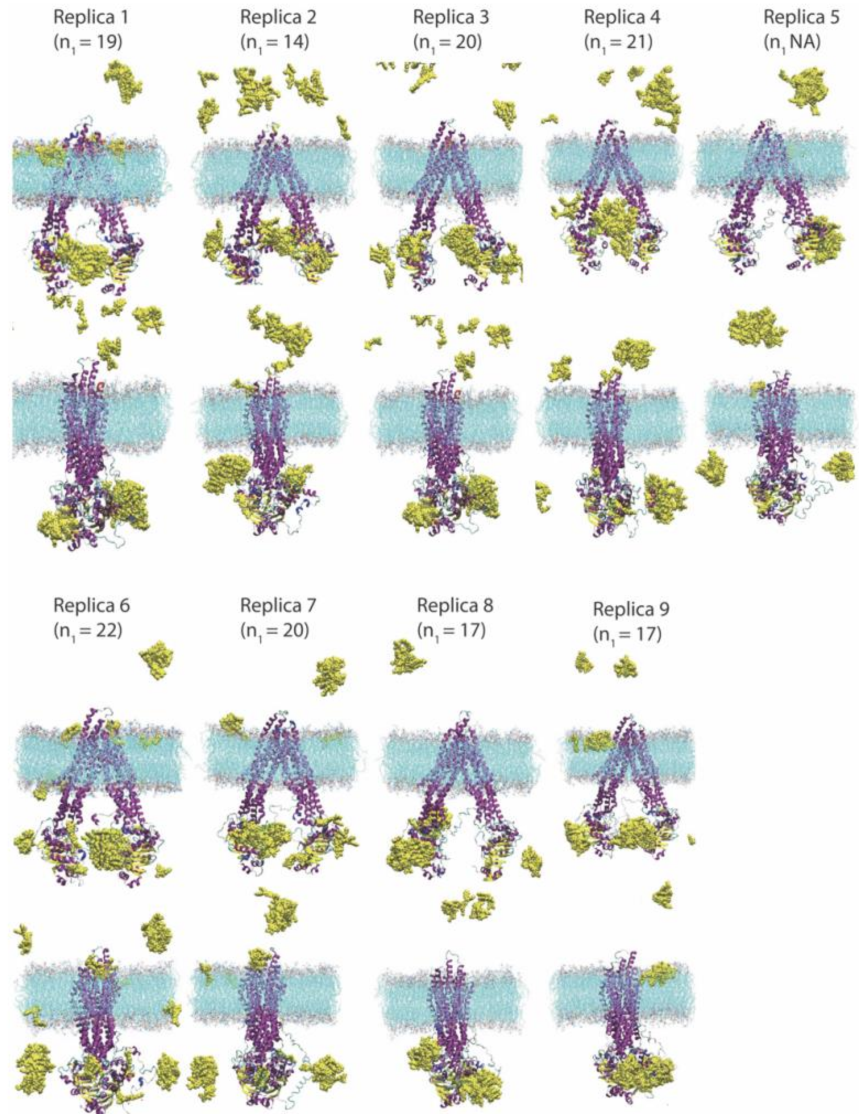

Sim. Specs

GROMACS 2020
CHARMM-36 ff
2.0 μs simulation
40 tariquidar in box

C. Jorgensen, M. B. Ulmscheider, P. C. Searson, *J. Med. Chem.*, **2023**, *66*

Inhibition of P-gp to prevent MDR

Replicates suggest tariquidar aggregation (19 ± 1) is an early stage in the inhibition mechanism

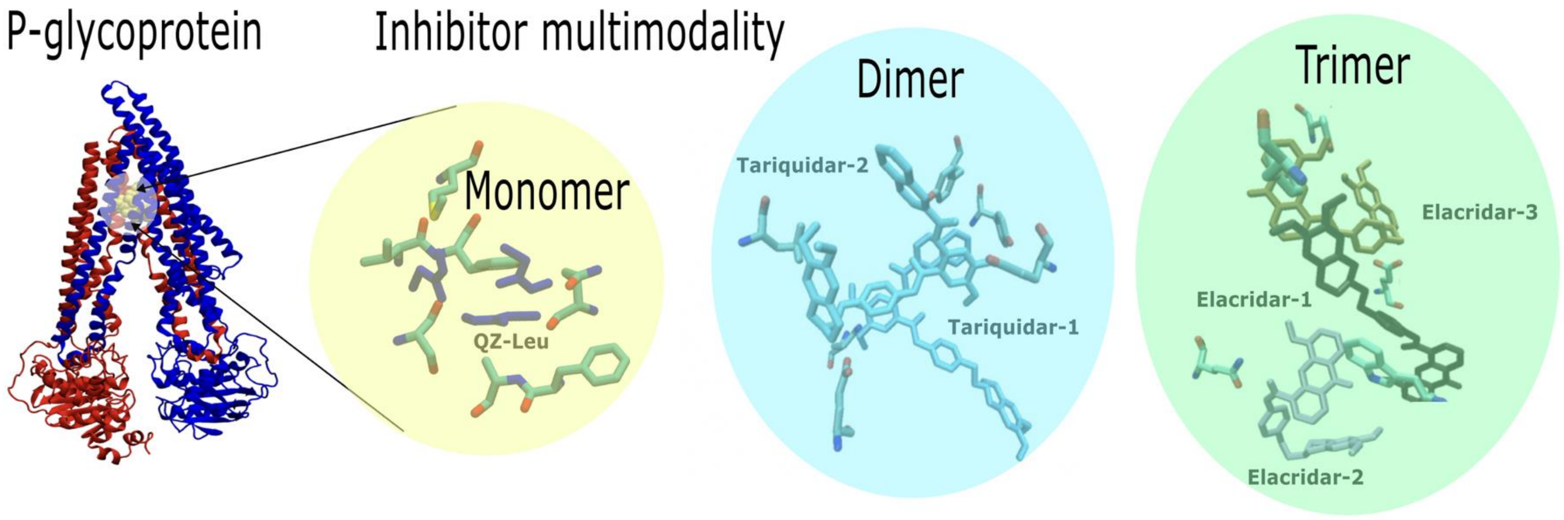

C. Jorgensen *et al*. *IJMS*, **2025** *26*(18), 9050.

Special Issue

Simulation and Artificial Intelligence Method Development for Complex Membrane Transport

Guest Editor

Dr. Christian Jorgensen

Deadline

10 May 2026

membranes

IMPACT FACTOR 3.6

Indexed in: PubMed

CITESCORE 7.9

C. Jorgensen *et al*. *IJMS*, **2025** *26*(18), 9050.

Verdict: BBB permeability models

- **Kramers-based methodology (1)** yields closest agreement to experiment but is a costly procedure.
- **Linear regression analysis (2)** yields sub 1 OM agreement. Larger library size needs to be considered
- Bayesian post-hoc corrected values from Adaptive Biasing Force, as well as **Steered MD permeabilities from Green-Kubo (3)** eqns. yield ~2 OM faster perm. wrt P_{app}

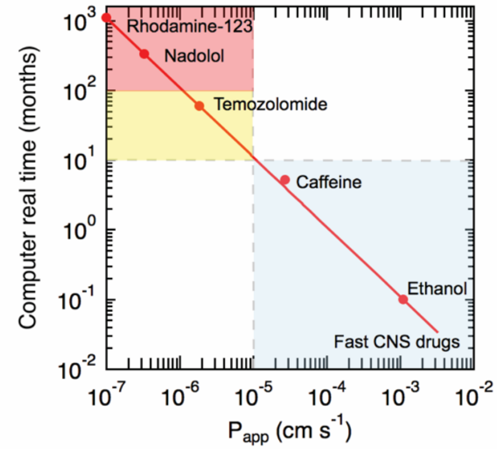

1. Kramers-based Arrhenius model Arrhenius extrapolation to 310 K with a correction in non-linear regime. Not routine.

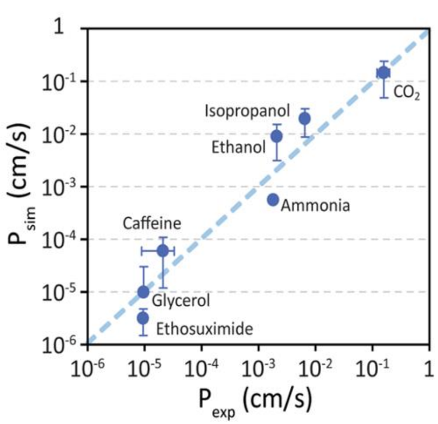

Wang *et al. Sci. Rep.*, **2019**

2. Regression based models Regression with high-T data. Accuracy to ~1-~2 OM on one GPU. Routine ranking of >10^1 molecules is now routine

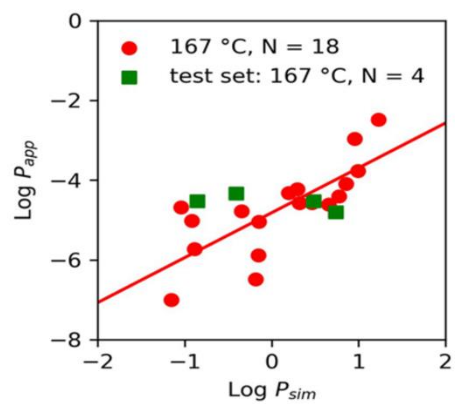

Jorgensen *et al. JCAMD*, **2023**
Jorgensen *et al*, *ACS Omega*, **2022**

3. Permeability via the Green-Kubo equations with steered MD

$$\frac{1}{P} = \int_{-d}^{d} \frac{\exp\left(\beta \Delta G(z)\right)}{D_z(z)} dz$$

$$D_z(z) = \frac{(RT)^2}{\int_0^\infty dt \left\langle \Delta F_z(z,t) \Delta F_z(z,0) \right\rangle}$$

Jorgensen *et al. JCIM*, **2025**